CHALMERS
UNIVERSITY OF TECHNOLOGY

Drone Arrestment System
Masters Degree project report

Concept Evaluation and Mechanical Dimensioning

Masters thesis project report in Mobility Engineering

Maxemilian Lundin
Theodor Schwarzmayr

DEPARTMENT OF INDUSTRIAL AND MATERIAL SCIENCE
CHALMERS UNIVERSITY OF TECHNOLOGY
Gothenburg, Sweden 2026
www.chalmers.se

Degree project report 2026

Drone Arrestment System
Masters degree project report

Concept Evaluation and Mechanical Dimensioning

MAXEMILIAN LUNDIN
THEODOR SCHWARZMAYR

Department of Industrial and Material Science
Chalmers University of Technology
Gothenburg, Sweden 2026

Drone Arrestment System Masters degree project report
Concept Evaluation and Mechanical Dimensioning
MAXEMILIAN LUNDIN
THEODOR SCHWARZMAYR

Supervisor: Magnus Evertsson, Department of Industrial and Material Science
Examiner: Magnus Evertsson, Department of Industrial and Material Science

Degree project report 2026
Department of Some Subject or Technology
Chalmers University of Technology
SE-412 96 Gothenburg
Sweden
Telephone +46 31 772 1000

Cover: CAD-Render visualizing the final design of the final prototype design of the degree project.

Typeset in LaTeX
Gothenburg, Sweden 2026

Drone Arrestment System Masters degree project report
Concept Evaluation and Mechanical Dimensioning
Maxemilian Lundin
Theodor Schwarzmayr
Department of Some Subject or Technology
Chalmers University of Technology

Abstract

Autonomous fixed wing drones have the potential to significantly improve maritime search and rescue operations by providing early situational awareness before rescue vessels depart. A central challenge for such systems is the reliable and autonomous retrieval of the drone after a completed mission. This thesis addresses that challenge by investigating and developing a mechanical drone arrestment system intended as a test platform for the Swedish Sea Rescue Society's autonomous drone program.
The work focuses on conceptual design, mechanical feasibility, and preliminary dimensioning of an arrestment system inspired by existing mid air recovery solutions. A capture concept based on a fixed hook mounted on the drone and a ground based string mechanism was selected and developed through iterative prototyping. Special attention was given to compensating for the roll motion typical of flying wing aircraft, as well as to handling the high mechanical loads generated during the arrestment event.
A kinematic model based on a cylindrical coordinate system was developed to describe the position of the capture string relative to the approaching drone. This model was used to guide the mechanical layout of the system and to support a proof of concept control approach. Several energy absorption concepts were evaluated, and a constant force band spring was selected as a compact and mechanically simple solution for controlled deceleration. Physical prototypes and preliminary structural analyses were used to assess geometric feasibility and to identify critical design constraints.
The outcome of the project is a mechanically viable arrestment system concept supported by analytical reasoning, CAD models, and prototype testing. Although full scale validation and closed loop control were outside the scope of the work, the results demonstrate that the proposed approach is feasible and provide a clear foundation for future experimental testing and system integration.

Keywords: drone recovery, arrestment system, fixed-wing UAV

List of Acronyms

Below is the list of acronyms that have been used throughout this thesis listed in alphabetical order:

UAV Unmanned Aerial Vehicle SSRS Swedish Sea Rescue Society

Contents

List of Figures

List of Tables

1

Introduction

1.1 Background

The project was initiated by SSRS, the Swedish Sea Rescue Society. Who are developing an autonomous drone system intended to get early eyes on scene when receiving distress calls at sea. The system is meant to be able to get visual information to the rescue crew before leaving the docks to be able to prepare accordingly to the situation at hand. By deploying a drone immediately upon receiving an alarm, real time visual information can be transmitted to rescue crews before they depart from the docks. This early situational awareness has the potential to significantly improve decision making, mission planning, and allocation of rescue resources, particularly in complex or time critical scenarios.

One important aspect and problem is retrieval of the drone after a mission. Since the organisation is a nonprofit organization and the rescue personnel are volunteers the drone system needs to be as autonomous as possible to avoid burdening the volunteers more than necessary. A manual retrieval could also limit the practical usefulness of the system since it increases the operational workload and diverting the attention away from the core rescue activites.

The drone that is currently planned to use for this type of mission can be seen in figure 1.1.The aircraft features a flying wing configuration, a design commonly used for small autonomous unmanned vehicles due to its aerodynamic efficiency, structural simplicity and low mass.

Since the drone platform is already developed and flight tested a constraint is to make minimal changes to the drone platform to not negatively affect the flight characteristics. Consequently, the design of the retrieval system must be adapted to the existing drone rather than the other way around. This constraint dictates the choice of capture method.

A company that already operates a comparable solution is Zipline, which maintains a fleet of fixed wing drones in Rwanda, delivering medical supplies between hospitals. Zipline's system is notable for its ability to recover drones in flight using a mechanical arrestment structure with only a hook on mounted to the aircraft.

SSRS has identified Zipline's solution as a relevant reference for its own autonomous

Figure 1.1: SSRS Flying Wing Drone mounted in launcher

drone operation. Although the operational context differs the underlying challenge of safely and repeatedly recovering aircraft drones remains similar. For this reason SSRS seeks to develop a test platform similar to Zipline's arrestment concept with the aim of evaluating capture feasibility, mechanical loads and system robustness under normal operation conditions.

1.2 Purpose

The purpose of the project is to design a subsystem of the drone project. The subsystem at hand is an autonomous drone retrieval system, which should be able to catch and allow for further processing of the SSRS drones autonomously without requiring manual intervention from rescue personnel.

1.3 Goals

This project aims to evaluate and design a system inspired by the company Zipline's solution of capturing drones from the air using a mechanical structure to decelerate and capture the fixed-wing drones. The end goal is to supply SSRS with a prototype design of a drone arresting system that can be used for further evaluation and testing. Furthermore the system should be compatible with the expected drone flight characteristics and environmental constraints, such as operation in maritime environments and variable weather conditions.

The final objective is to deliver a test platform concept to further develop the idea through real world testing and potential integration into SSRS's drone system. This includes identifying key design challenges.

1.4 Limitations / Demarcations

- Focus will remain on the mechanical capture structure and its integration with drones
- The project will only develop software for proof-of-concept and knowledge gain
- The project will not entail any simulation of control systems

2

Theory

2.1 Coordinate system

Due to the behavior of a flying wing drone which causes it to continuously roll to keep its course the solution for catching the drone needs to be able to account for the roll of the drone. The drone catcher also needs to be able to convert between the coordinate system of the drone catcher and the drone to make sure future work of the control system will be able to use a single coordinate system.

The solution uses two servos/stepper motors to allow independent rotation of two arms, where a string is fastened between the ends of the arms.
What is of interest to the function of the system is the positioning of the string, both in terms of height, rotation around the structures axis and the angle in the axis of roll for the drone. That means that the drone catcher should be able to compensate its own positioning depending on the flight altitude, direction of approach and roll of the drone.
The theoretical basis for the solution is translating the solution into a cylindrical coordinate system, where two circles of a radius equal to the radius of the radial extent of the tips of the arms on the drone catcher (squared with red color in figure 2.1). The distance between the two circular paths is equal to the distance between the tips of the arms. A vector is drawn between the two points which represents the position of a string between the arms. This is illustrated in figure 2.1.

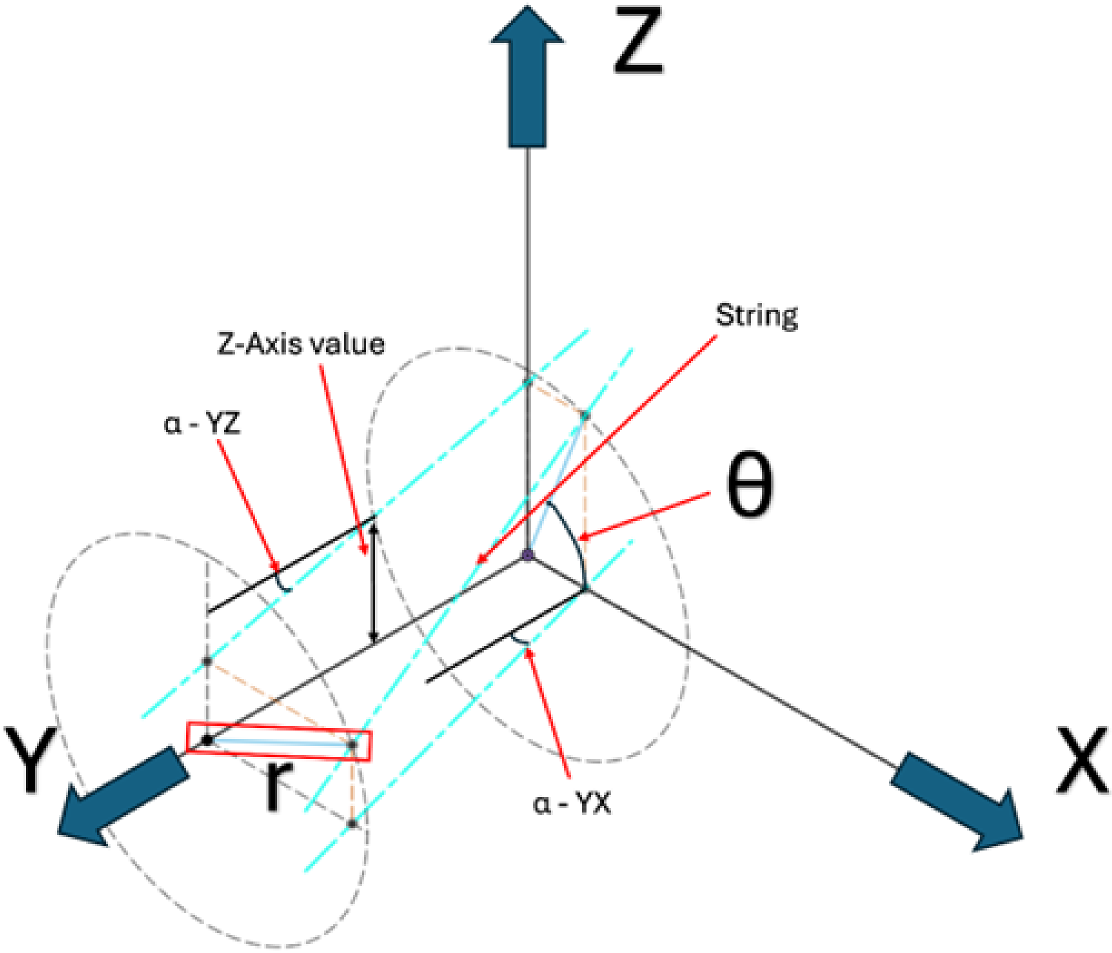

Figure 2.1: Illustration of a cylindrical coordinate system with the cartesian coordinate system used for the drone

To be able to determine the roll angle of the vector, an orthogonal projection of the vector is made onto the YZ-plane, the angle of the projected vector with respect to the Y-axis will then be the same as the roll angle of the drone.
An orthogonal projection can also be made onto the XY-plane to find out how much the positioning requires compensation in the rotation of the solution, as changing the YZ-angle will result in the projection on the XY plane rotating, which will require the solution to compensate by rotating the cylindrical coordinate system to stay orthogonal with the drones coordinate system.
The height of the drone is compensated for by evaluating the Z-axis value of middle of the projected vector in the YZ-plane.

The control actuators available in the solution is a servo motor for each arm, and a servo motor to rotate the base of the solution, which results in a rotation of the cylindrical coordinate system.
To calculate the angles of the servomotors in order to get the correct values we will have as inputs:

- YZ-angle (roll angle)
- Z-axis value (altitude of the drone)

With these values we will need to calculate the azimuth angles on the two circles, this calculation will have 2 possible results, but the results will be limited to angles between $0 - 90°$ which limits the solutions to one for most cases.

2.1.1 Assumptions

To enable analytical treatment of the drone arrestment problem, a number of simplifying assumptions are introduced. These assumptions are intended to support preliminary dimensioning and conceptual evaluation rather than to fully describe real world behaviour. Since the system is designed as a test platform, several parameters are expected to be refined through experimental validation.

The approach conditions of the drone during capture are difficult to determine in advance and are expected to vary depending on environmental factors such as wind, turbulence and navigation accuracy. For this reason, no strict limits are imposed on the flight state at the time of capture. It is assumed that the drone approaches the arrestment system within a reasonably repeatable corridor in position and attitude such that capture is possible. The acceptable limits of approach speed, roll angle and lateral offset are therefore treated as unknowns to be investigated through future real world testing.

The capture string is assumed to be a fishing line with negligible mass compared to the drone and the arrestment structure, and is therefore treated as massless. The string is pre tensioned to a force of approximately 72 N, corresponding to the nominal force level of the selected band spring. The string is assumed to behave as an inelastic element that can only carry tensile load.

The arresting arms are not assumed to be perfectly rigid. However, their stiffness is considered sufficiently high that elastic deformation of the arms is small compared to the compliance of the shock absorption system. For the purpose of global force and energy analysis, the arms are therefore treated as rigid bodies.

During the arrestment event, the drone is modelled as a lumped mass undergoing deceleration primarily along its direction of flight. Rotational effects of the drone and secondary force components are neglected in the initial analysis. The main deceleration is assumed to occur after successful engagement between a hook and the capture string.

Aerodynamic forces acting on the drone during arrestment are expected to be significantly smaller than the mechanical forces generated by the arrestment system. Their influence is therefore discussed qualitatively rather than included directly in the analytical force calculations.

2.1.2 Deceleration Theory of the Drone

When the drone engages with the capture string, its kinetic energy must be absorbed by the arrestment system. The drone is modelled as a lumped mass undergoing one-dimensional deceleration along its flight direction. Aerodynamic forces are small in comparison to the spring forces and are therefore neglected.
The kinetic energy of the drone at the moment of capture is

$$E_k = \frac{1}{2} m v_0^2 \tag{2.1}$$

where m is the drone mass and v_0 is the approach velocity.
For the design case

$$m = 0.9 \text{ kg}, \quad v_0 = 12 \text{ m/s} \tag{2.2}$$

the kinetic energy becomes

$$E_k = \frac{1}{2} \cdot 0.9 \cdot 12^2 = 64.8 \text{ J} \tag{2.3}$$

This energy must be dissipated through mechanical work performed by the capture string and the constant-force band spring.

Geometric Force Model

After engagement, the drone pulls the string into a symmetric V-formation between two mounting points separated by a distance d. The half-spacing is

$$r_0 = \frac{d}{2} \tag{2.4}$$

As the drone moves forward a distance x, the length of each string segment becomes

$$L(x) = \sqrt{x^2 + r_0^2} \tag{2.5}$$

The extension of each string segment relative to its initial length is

$$s(x) = L(x) - r_0 \tag{2.6}$$

For a constant-force band spring with constant tension T, the horizontal resisting force acting on the drone is given by the horizontal components of the two string tensions,

$$F(x) = 2T \frac{x}{\sqrt{x^2 + r_0^2}} \tag{2.7}$$

The resisting force increases with displacement due to geometric alignment of the string with the flight direction.

Energy Balance and Stopping Distance

The drone stops when the work performed by the resisting force equals the initial kinetic energy,

$$\int_0^{x_{\text{stop}}} F(x)\,dx = E_k \tag{2.8}$$

Evaluating the integral gives

$$W(x) = 2T\left(\sqrt{x^2 + r_0^2} - r_0\right) \tag{2.9}$$

Setting $W(x_{\text{stop}}) = E_k$ yields the stopping condition

$$2T\left(\sqrt{x_{\text{stop}}^2 + r_0^2} - r_0\right) = \frac{1}{2}mv_0^2 \tag{2.10}$$

Solving for the stopping distance gives

$$x_{\text{stop}} = \sqrt{\left(r_0 + \frac{mv_0^2}{4T}\right)^2 - r_0^2} \tag{2.11}$$

The maximum extension of each string segment becomes

$$s_{\text{max}} = \frac{mv_0^2}{4T} \tag{2.12}$$

The geometric nature of the string arrangement results in a nonlinear force– displacement relationship. The resisting force increases monotonically with displacement as the string aligns with the flight direction. This behavior is illustrated in Figure 2.2. And the theoretical force to displacement can be viewed in figure 2.3.

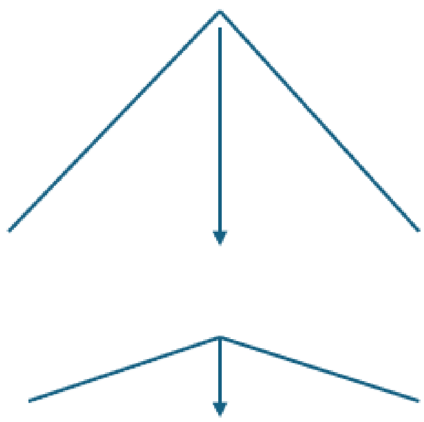

Figure 2.2: Illustratrative free body diagram of the force to displacement of the string

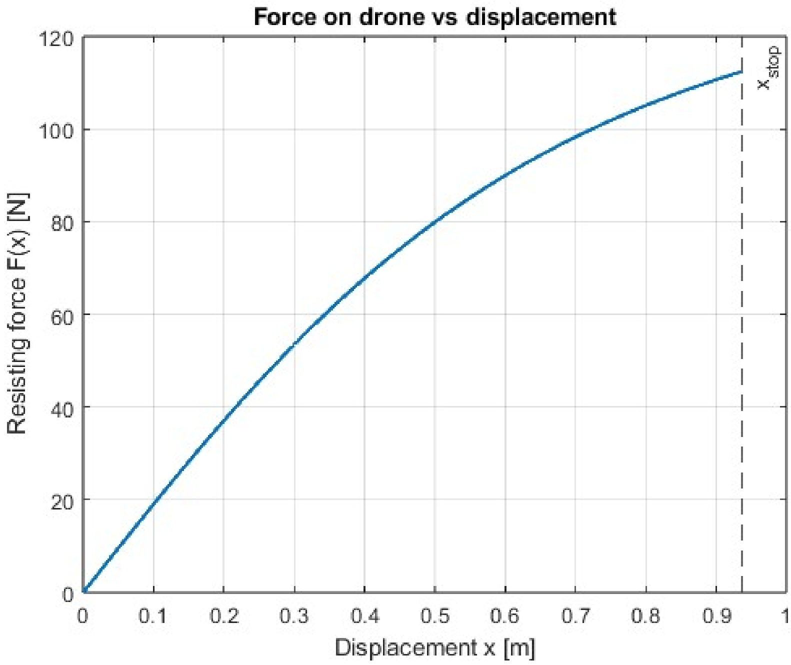

Figure 2.3: Theoretical resisting force as a function of drone displacement.

The time-dependent deceleration behavior follows from integrating the equation of motion

$$m\ddot{x} = -F(x) \tag{2.13}$$

which yields a nonlinear deceleration profile. The resulting acceleration response is shown in Figure 2.4.

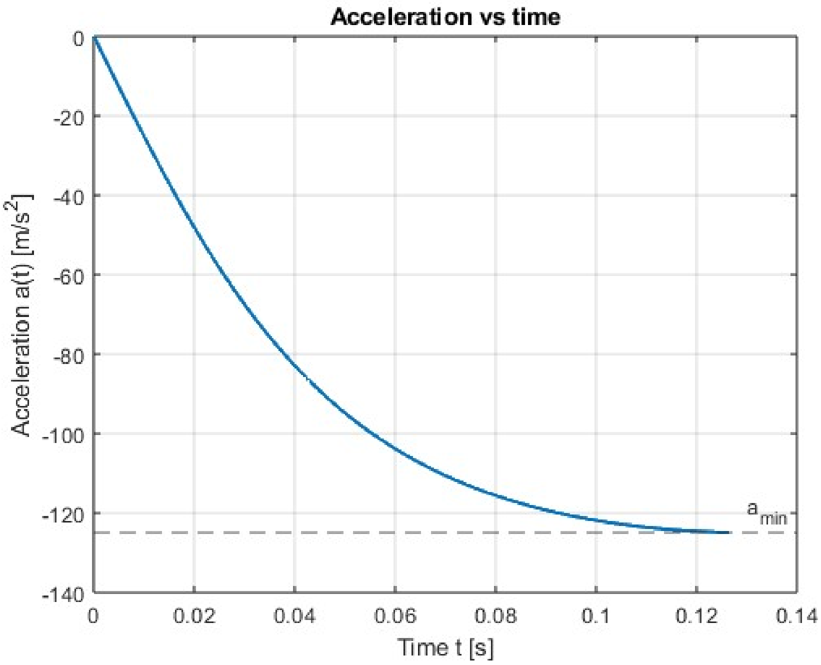

Figure 2.4: Theoretical acceleration of the drone during arrestment.

The nonlinear shape of both curves arises purely from geometric effects, as the band spring force itself remains constant.

3
Methods

The product development method used in this project is mainly a rapid prototyping process, in which the goal is to continuously design, manufacture and test parts of a design in order to understand the strengths and weaknesses the design possesses. The methods used for testing will differ a lot depending on the specific part that is being developed. However the requirements are always based on the functional model of the system, and the strengths and weaknesses that every iteration has are documented and quickly rated to determine if the weaknesses are able to be designed around.

3.1 Prototyping Approach

To begin gaining insight into the problem and developing an understanding of the product, the first objective was to build a scaled prototype. This process started with discussions and evaluations of several conceptual solutions. Prototyping an incomplete or simplified version of the product early on proved valuable, as it generated substantial knowledge and helped establish design criteria for the final system.

Once a concept was selected, several design iterations were created and 3D-printed to serve as a test bench. In addition, early exploration of the software interface and functionality was initiated. This step was highly valuable, as it provided further understanding of system requirements and revealed additional constraints and opportunities relevant to the mechanical design.

3.2 Testing and Validation

To test the concepts focus was put on the critical components and a wide variety of testing methods were used during the project. The first prototype was made mainly to gather information about the problem. This prototype was also used in combination with some cheap radio control hobby servos and an Arduino pro micro to develop the embedded code for the system. This code is unfinished and very crude, made mainly for gathering more information about the product and the problem.

3.3 Software and Controls

3.3.1 MAVLink Integration

Communication between the drone flight controller, onboard processors, and ground control systems was handled using the MAVLink protocol. MAVLink provides a lightweight and robust message-based communication standard widely used in unmanned aerial systems. It was employed to transmit telemetry data such as attitude, position, airspeed, and system status, as well as to send control commands and configuration parameters. Using MAVLink enabled seamless integration with existing tools and facilitated debugging and logging during both simulated and experimental tests.

3.3.2 Mission Planner

Mission Planner is a open source ground control software widely used for configuring, simulating, and monitoring unmanned aerial vehicle (UAV) missions. It provides an interactive environment, shown in figure 3.1, in which flight missions can be defined using waypoints, flight modes, and mission commands, allowing users to visualize planned trajectories and expected vehicle behavior before execution. In addition to mission planning, the software includes a simulation mode that emulates vehicle dynamics and autopilot logic, enabling preliminary evaluation of mission flow, waypoint transitions, and timing without the risks associated with real-world testing. As such, Mission Planner serves as a practical tool for gaining insight into overall mission logic and flight behavior during early stages of system analysis and design.

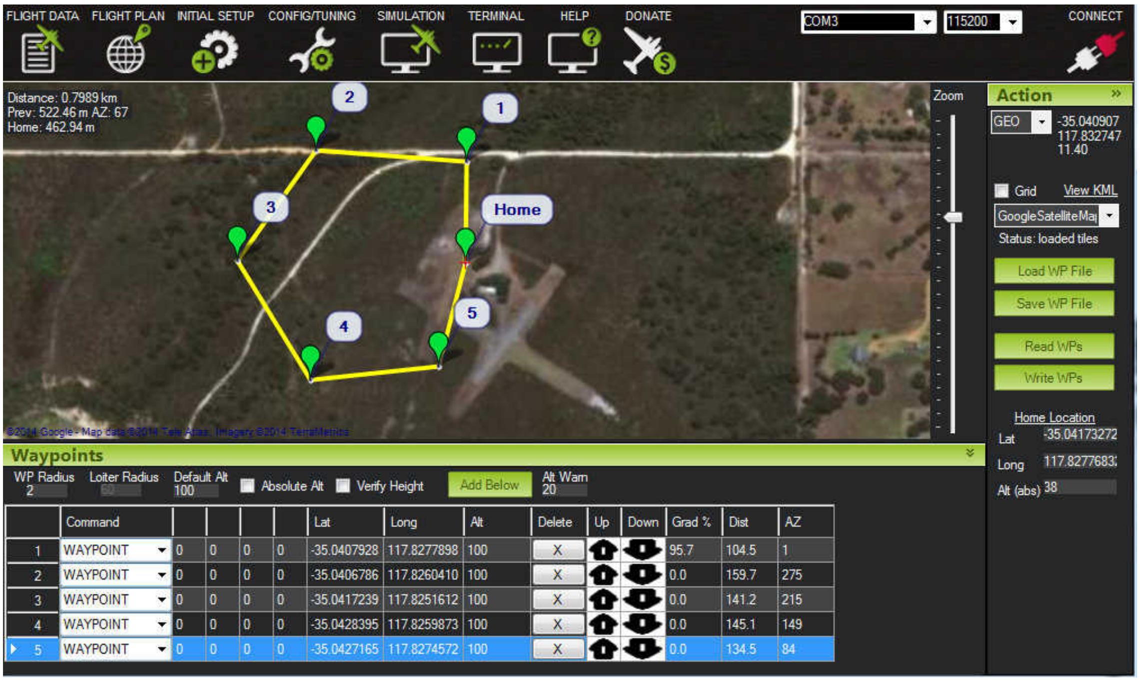

Figure 3.1: Mission Planner Open Source Software interaction display

By simulating representative way-point missions in the Mission Planner environment, the general flight behavior and mission logic of the drone could be studied. While the simulations did not provide a reliable estimate of the approach velocity during a capture maneuver, they were useful for understanding flight path predictability, waypoint transitions, and overall mission timing.

In addition to simulation, flight data from real-world test flights was obtained and analyzed. This data reflected operation under realistic environmental conditions and provided valuable insight into achievable flight speeds and stability limits. Based on this data, and observations from flight testing, the minimum speed for stable flight was estimated to be approximately 12 m/s. This value was therefore used as a design assumption for subsequent analysis of the capture mechanism.

Although the simulation environment offered the potential for more detailed analysis, such as systematic variation of mission parameters and environmental disturbances, the scope of this work was limited by time constraints. As a result, the simulations were primarily used for qualitative understanding rather than exhaustive optimization.

Some of the further capabilities of Mission Planner is to incorporate the external electronics and testing to see if the control systems work as intended. This could help in monitoring input signals and communication between the ESP32 micro controller and the on-board drone software. An example of this could be simulating when the drone is nearing a arrestment station where the platform should start rotating to face the drone. A telemetry radio can also be incorporated into this simulation, using every part of the system except the drone making testing much easier and less cumbersome.

3.4 System Integration Context

The drone should be launched by the launcher that already exists. After this the mission is executed and the drone returns to the base where the drone arrestment system secures the drone and puts it in a charging station to make it ready for the next mission. This arrestment system should fit into a larger system that does not yet exist. This means that there are many uncertain variables that might change the final design. Though this is a step in the right direction towards a complete system.

The arrestment system is communicating with the drone when in range for the telemetry radio and only directly controls the drone after the string is secured in the hook. After this critical step the drone could be put in some sort of charging bay and unhooked from the string to prepare it for the next launch. This step would also include transporting it back to the launcher.

3.5 Requirements and Specifications

3.5.1 Critical Constraints

To get started with the design and to explore if it is at all viable the critical components were identified and analysed. How the critical components are defined is through the functional diagram and using the current concept to find the weaknesses. When a weakness is identified such as the line arresting the drone, it is analyzed to see if there are viable options on the market holding up to the forces or if there is another better solution to the problem.

3.5.2 Functional diagram

To provide a structured overview of the system and its intended behavior, a functional diagram was developed, as shown in Figure 3.2. The purpose of the functional diagram is to describe what the system must do, independent of how the functions are physically implemented. This abstraction helps to ensure that all required system functions are identified and that their interactions are clearly understood before detailed mechanical and software design decisions are made.

The diagram decomposes the drone arresting platform into a set of core functions and illustrates the flow of energy, information, and mechanical interaction between them. The primary function of the system is to detect, intercept, and arrest a moving aerial vehicle in a controlled manner. This general function is supported by several subordinate functions, including state estimation and sensing, control and decision-making, actuation, and energy supply.

Sensor inputs provide information on the position, velocity and timing of the incoming drone, which is processed by the control system. Based on this information, control commands are generated and transmitted to the actuators. These actuators convert electrical energy into mechanical motion, allowing the arresting mechanism to move into position and physically interact with the target drone. The mechanical forces generated during arrest are transferred through the structure and dissipated or managed to prevent damage to the system.

The functional diagram also highlights the interaction between hardware and software components. Communication links and feedback loops are included to represent telemetry, control feedback, and system monitoring. By visualizing these relationships, the diagram served as a reference throughout the development process, supporting requirement definition, prototype testing, and iterative refinement of both mechanical and control-related subsystems.

Overall, the functional diagram acted as a central tool for aligning system requirements with design decisions and for identifying critical interfaces and constraints early in the development process.

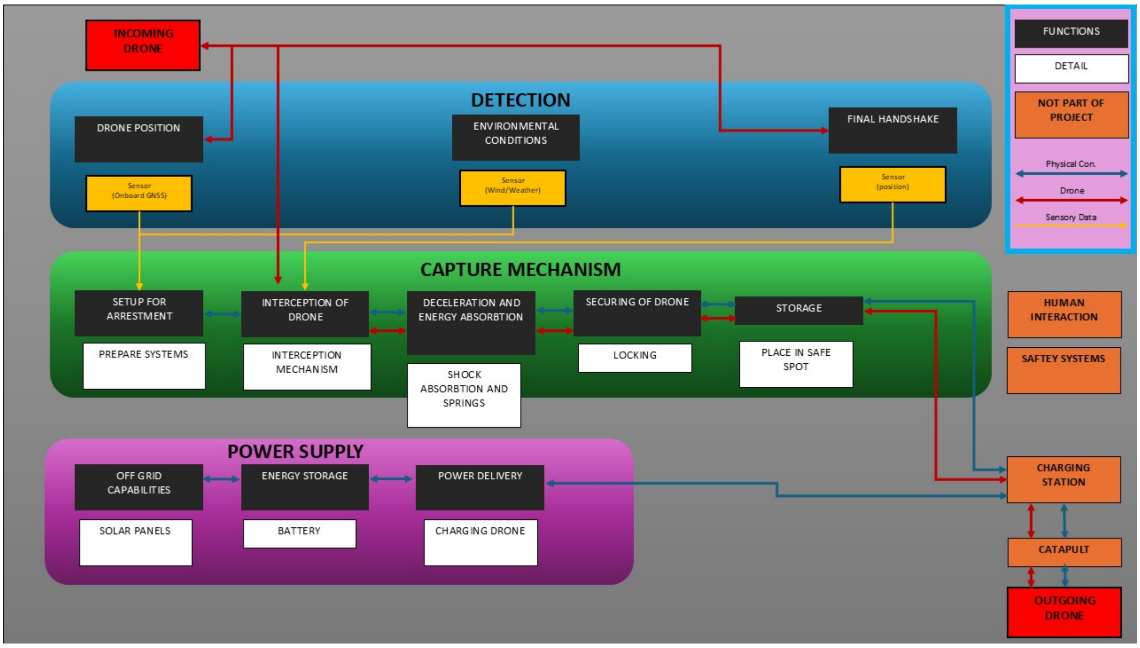

Figure 3.2: Functional diagram of the entire drone arrestment platform

3.6 Concept Development

The first step made in the concept development was to determine what kind of setup was to be used. A pre-study on what solutions already exist was made. As well as a few possible concepts were generated based on possibilities of integrating them with the already set design of the drone and launcher system.

3.6.1 Capture system

A few different solutions for the capture mechanism of the drone were considered, most were quickly ruled out due to being non realistic in practice. The following table will quickly list some of the considered solutions and pros and cons to why or why not to use the solution:

Concept	Pros	Cons	Usefull (Y/N)
Fixed Hook and String	Little Risk of damage to aircraft, Easy autonomous release possible, Can be designed to fit with launcher	Adds parts/weight on the drone	Y
Trailing hook and String (Zipline solution)	Very low risk of damage to drone, proven solution	Hard to integrate with launcher, Hard to autonomously release, Risk of getting caught in propeller	N
Chute/Funnel	Very easy autonomous reload of drone/ does not require releasing after catching	High risk of damage to drone if approach angle is slightly off.	N
Net	easy to capture drone without extra hardware on drone	Big risk of getting tangled if net is loose, hard to position drone post interception if net is stiff	N
Robot Arms with suction cups (Earlier final solution for this project)	No extra equipment on drone	Requires precise control of capture system and state estimation of drone	N

Table 3.1: Capture system

The selected capture system was determined to be a fixed hook on the drone and a string on the capture device.

3.6.2 Overall capture system layout baseline

With the capture system selected the next step is to determine the layout of the capture system. To determine the most suitable layout a combination of rapid prototyping and market research was used. The pros and cons of the market research have been made in short form in table 3.2.
For a more thorough explanation of the market research concepts, please see A.1.
The candidates for the market research are Zipline, Boeing Skyhook and Heishatech F200. As little is known abut the Heishatech solution and the fact that the working principle is very similar to Zipline they are lumped together in table 3.2

Concept	Zipline (Baseline)	Boeing Skyhook
Control Simplicity	/	+
Post- catch handling	/	-
Stress on Drone	/	-
Result	0	-1

Table 3.2: Illustrative matrix for baseline system layout selection

The baseline concept selected was the Zipline design.

3.6.3 Iterative development of layout

3.6.3.1 First iteration parallel swing model

With the baseline concept selected, a basic early concept was made using CAD software, with animations to show the function of the system shown in figure 3.3. This concept was heavily inspired by the company Zipline's solution in Rwanda.

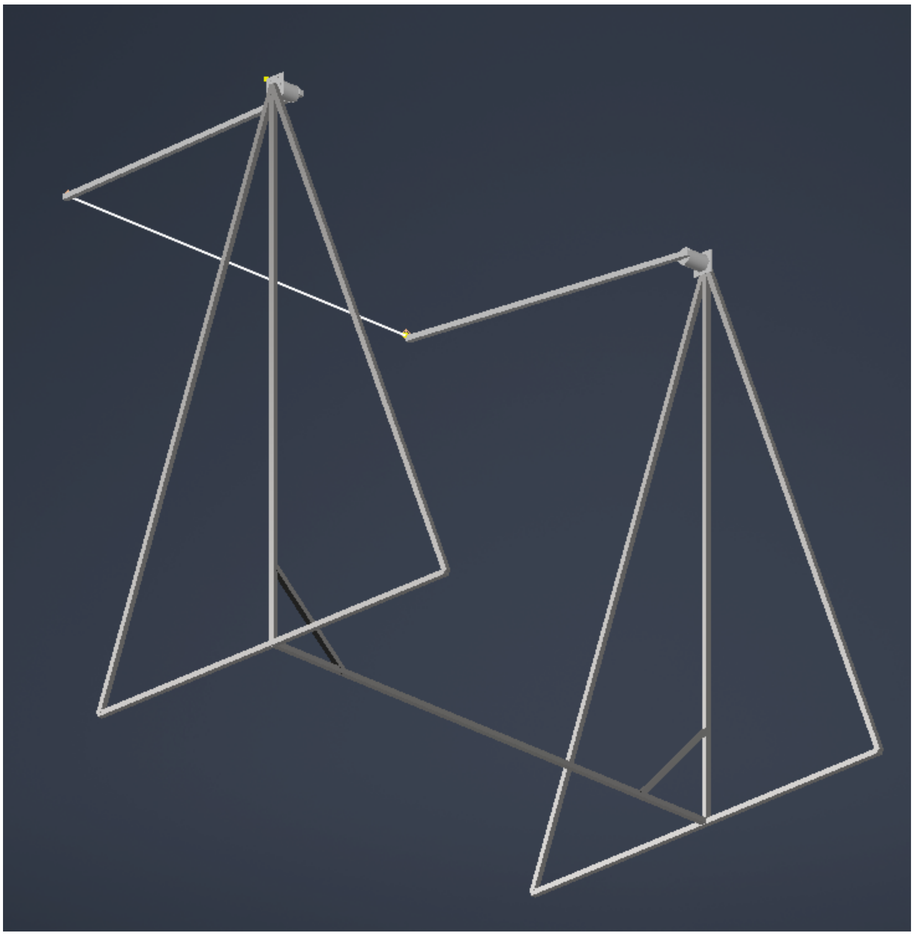

Figure 3.3: CAD model of first iteration

The main takeaways from this iteration was a requirement to be able to rotate the contraption against the wind direction, to make the ground speed as low as possible.

Due to this a couple of changes need to be made to the concept, as the concept is big and bulky which would make rotating the whole structure cumbersome. This concept would also need the drone to be stable enough to not hit the structure. Also it would be impractical to setup and transport for testing in the real world. Some more insights are that the load case for the motors and the rotating arms are better in this concept compared to the latter ones but it was decided that this could be designed around after some investigation.

3.6.3.2 Second iteration V-formation single motor model

The next iteration placed the bulk of the weight in the center of rotation of the contraption. Using only one motor to move the catching arms. The catching arms attach to the central platform which itself can be rotated using one motor. The CAD model can be seen in figure 3.4 and a 3D-printed version can be seen in figure 3.5

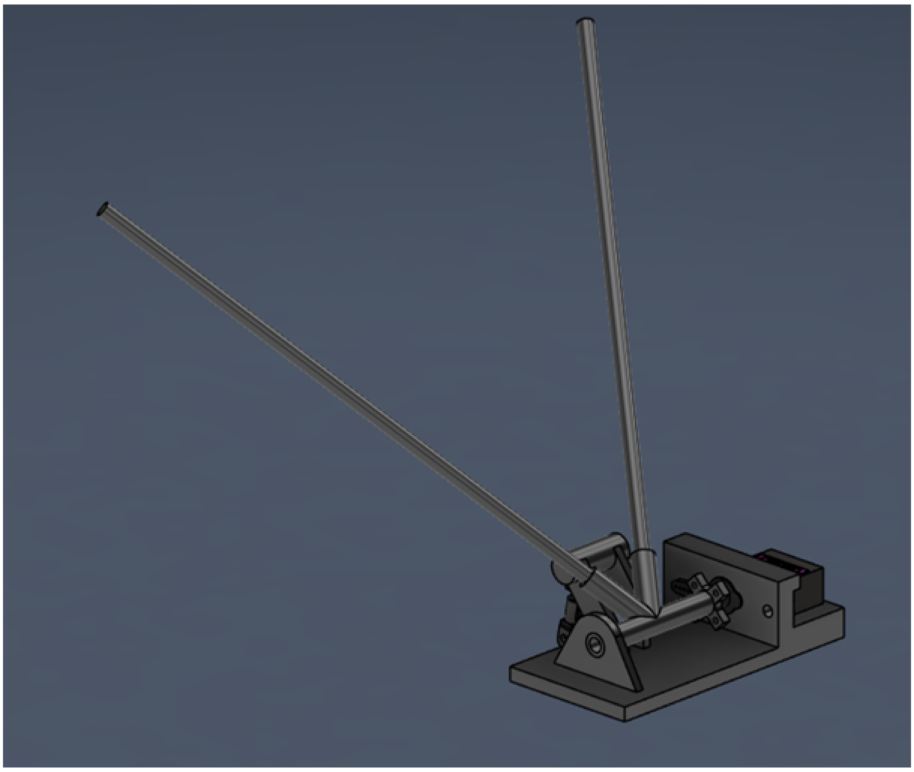

Figure 3.4: CAD view of second iteration

This concepts main drawbacks where the bending of the catching arms, which requires some solution. Different solutions were brainstormed, the main ones being a steady rest with a spring to dampen and support the arms. Another solution was to add damping to the catching string itself. It was determined that the damping solution would require further work, but was not deemed critical at this point in the project.
This design was 3D-printed at a smaller scale to evaluate the design in a more hands on way. And was used to start developing a control system for more in-depth evaluation of requirements.

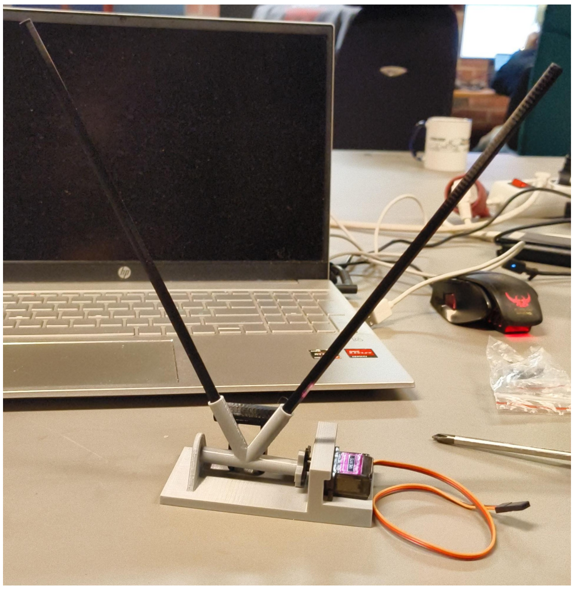

Figure 3.5: 3D-printed version of the second iteration

While working with the control system the drones were noticed to have a sinusoidal roll pattern, which would make catching the drone harder. If the drone is at a roll angle at the moment when it is caught the string will hit the wing instead of latching with the hook. This was the main driving requirement to allow for in the next iteration.

3.6.3.3 Third Iteration V-formation double motor model

The third iteration aimed to allow for roll offsets in the drone while being caught. The way this was solved was by splitting the arm rotor axle into two as shown in figure 3.6. And adding a motor as to make each arm individually controllable.

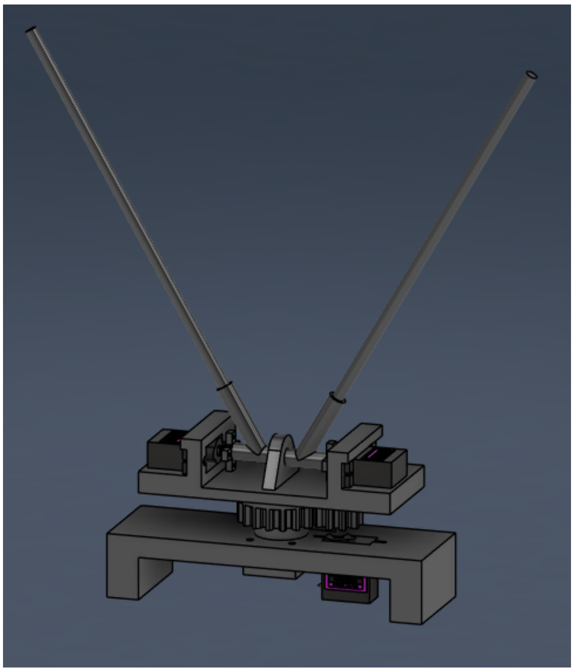

Figure 3.6: CAD model of third iteration

For the third iteration a 3d-printed mockup was made, figure 3.7, and a proof of concept control system based on the coordinate system in 2.1 was made.

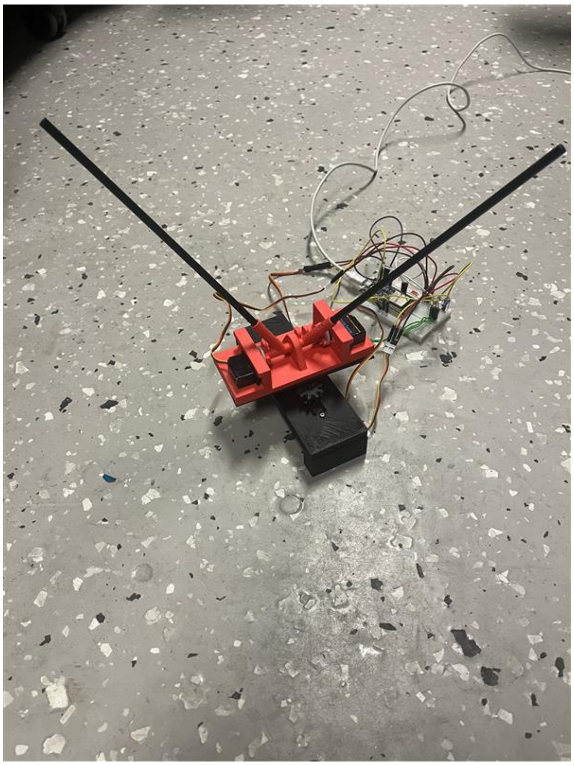

Figure 3.7: 3d printed prototype of 3rd iteration

At this point in the project the concept was deemed mature enough for further detailed design work.

3.6.4 Control system and Software

In parallel with developing the mechanical arrestment concepts a control system architecture was investigated to expand the project. This was not part of the plan initially but in order to get a good understanding of the project it was decided to work on a basic implementation, allowing for mechanical and software design decisions to inform each other early in the process.

To start this development an Arduino was used to control the motors to catch the drone. The Arduino platform was chosen because of availability and simplicity. In the first concept iteration, a single motor was considered sufficient to actuate the arresting arms. However, early testing and geometric analysis showed that independent control of the left and right arms was required to robustly capture a flying-wing drone, particularly under non-zero roll angles during approach. As a result, the system was redesigned to use two independently controlled motors, allowing asymmetric arm positioning.

To incorporate this the mathematical model in the theory chapter was used to calculate the angle and position of the arms based on the flying altitude of the drone and the roll angle. These values are sent from the drone to the arresting system through a telemetry radio. In the future it might be possible to send this data over 4G/5G cellular network that is already installed on the drone, but this would require testing over different latencies to get the timing correct and verify feasibility. For testing a normal telemetry radio can be used to get low latency data of these parameters.

3.7 Detailed Mechanical Design

3.7.1 Energy Absorption

For the energy absorption mechanism a preliminary calculation for the required energy to be absorbed was conducted, see 2.1.2. No matter what, the deceleration distance needs to be around one meter long, and not more than one and a half meters long. As going longer for deceleration would lead to the possibility of hitting the ground before stopping in some cases. And the drones are already being accelerated from standstill to flight speed in about one meter. Which means that a similar deceleration should not risk causing damage to the drones.
The concepts will be briefly explained in this chapter.

3.7.1.1 Energy absorbing steady rest

One early concept that was considered was a steady rest and shock absorber design. The main positives of this design is the reduced moment reaction in the arms. The way it would function is that the arms would fall onto the steady rest during capture as is illustrated in figure 3.8. The steady rest would then work to absorb the energy of the drone, this would lead to a much simpler string setup. This design however also comes with many drawbacks.

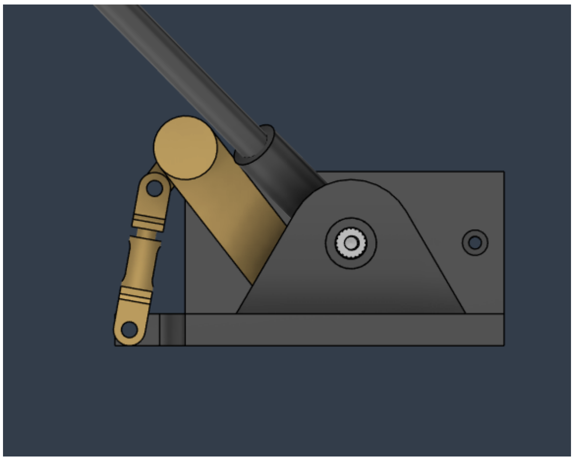

Figure 3.8: Early concept with steady rest and shock absorber in yellow

One main problem is that the damping has to be well dimensioned to make sure that the rods do not act as springs themselves, which could cause the catcher to loose the drone.

Another problem is that it becomes difficult to implement with the dual motor setup, as the string would need to be able to change length. This would cause the simplicity of the design to be neglected completely, as another string length compensation system would be required.
This design also has the positive aspect of acting as a braking system, which make sure that a separate brake is not required in conjunction, which most other concepts do.

3.7.1.2 Spring and string length compensator

The spring and string length compensator solution would incorporate only energy absorbtion of the string. This would be done by using a spring that adheres to Hookes law. And to make sure that the string force is predictable no matter the position of the arms, a string compensator would be driven directly by the two shafts to make sure the string is always at the same baseline tension.

The positives of this design is that the constantly increasing spring force would make sure that the drone does not risk over-travel while decelerating. While still being able to keep the impact force low on the hook device on the drone.

The negative part of the design is that it requires a string length compensator. This proved to be difficult to do without adding friction that would worsen and risk braking the compensator. A few different iterations of a string compensator were designed. But none worked well enough to be worth pursuing.

3.7.1.3 Gas spring

Using a gas spring would address many of the problems with using a normal compression or tension coil spring and a string length compensator. As gas springs have a rather constant force it would not need to use a compensator. A gas spring also has better damping behaviour than normal springs, which the system could benefit from. The negative part is that a lot of force reduction by use of a gearbox or similar would be needed. One simple solution for the gearing issue would be too use a series of pulleys to reduce the force and increase the amount of string displacement possible. This would be reasonably easy to manufacture, and for testing of a prototype it would be possible to try many different gear ratios to find a good sweet-spot. As it is easy to bypass or add extra pulleys. However it would lead to some extra friction, and the solution would still take up a lot of space. The solution was considered far enough to where more detailed designs were created and iterated as can be seen in figure 3.9.

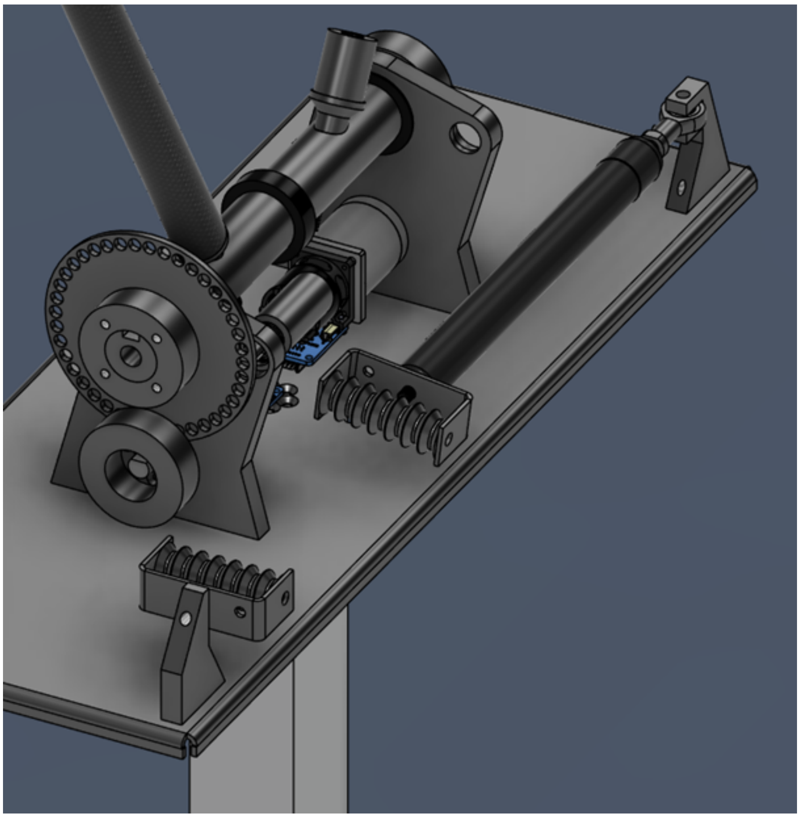

Figure 3.9: Gas spring with pulleys

The solution should be possible to use. But due to the large amount of pulleys required, the reliability and simplicity of assembly and use would be lacking.

3.7.1.4 Constant force band spring

Mainly due to the amount of gearing required for the gas spring to work, a concept using a constant force band spring was considered. The main positives with a band spring is that it can be built very compact and with very few components. This makes installation and packaging easy, and the part is only a small module that can be placed rather arbitrarily as can be seen in figure 3.10.

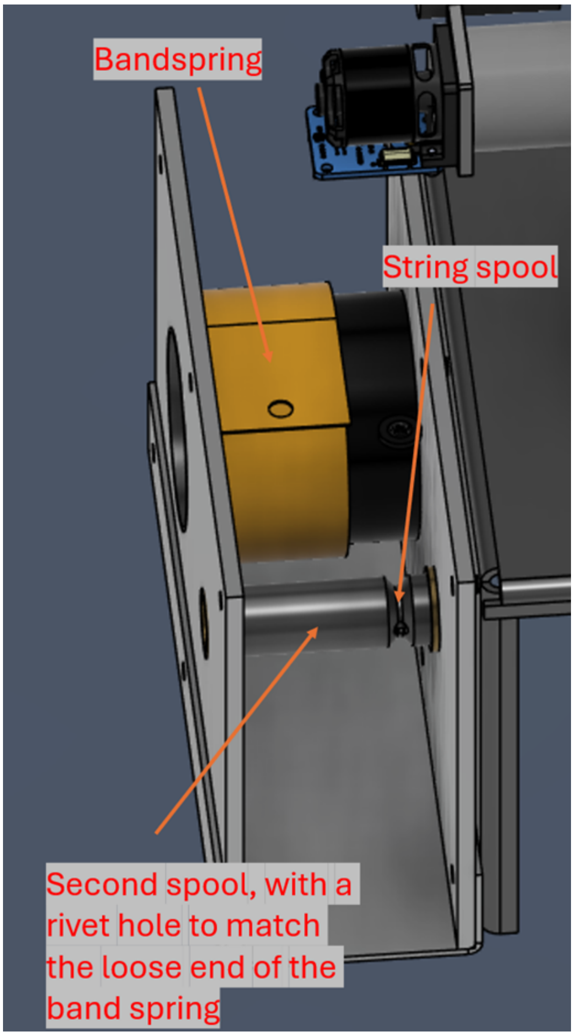

Figure 3.10: Band spring Module with top cover removed

Band springs are also available in many different force ratings, which makes dimensioning easy. A negative aspect of the band spring is that it does not have the same damping quality as a gas spring. A solution to this is to design in some friction into the system which could dampen oscillations.

The band spring concept would work by having two spools, one with the band spring being able to rotate freely and another with a rotor that can spin freely. The loose end of the band spring would then be fastened to the free rotor and get spooled up on the free rotor. On the free rotor a string would also be wound which would allow for a basically arbitrary amount of string displacement by use of different active spool radii between the band spring input and the string output spool. Since band springs allow for highly customizable of displacement lengths and force ratings, this design will aim to keep a equal radius on both spools.

Dimensioning calculations for the band spring system can be found in A.2.3.

3.7.2 Locking

To ensure reliable retention of the drone after interception, a dedicated locking mechanism is required at the interface between the drone-mounted hook and the arrestment string. An initial concept based on a passive open hook was considered. While such a solution is mechanically simple, it presents a significant risk of unintentional release due to rebound effects during the initial deceleration phase. As the arrestment system stores elastic energy, oscillatory motion of the string may cause the hook to disengage if no positive locking feature is present.

To mitigate this risk, a spring loaded latch mechanism was developed shown mounted on the drone in figure 3.11. The latch is designed to automatically close once the string enters the hook geometry, providing positive mechanical retention throughout the deceleration and post locking phases. This ensures that transient load reversals or oscillations in the shock absorption system do not result in loss of capture.

In order to guide the arrestment string into the latch opening and reduce the risk of interference with the drone's winglets, a guiding ramp is integrated into the hook assembly. The ramp provides a smooth lead in surface that directs the string toward the latch even if the drone roll angle is a little misaligned to the arrestment system. This feature increases capture robustness and relaxes alignment requirements for the approach trajectory.

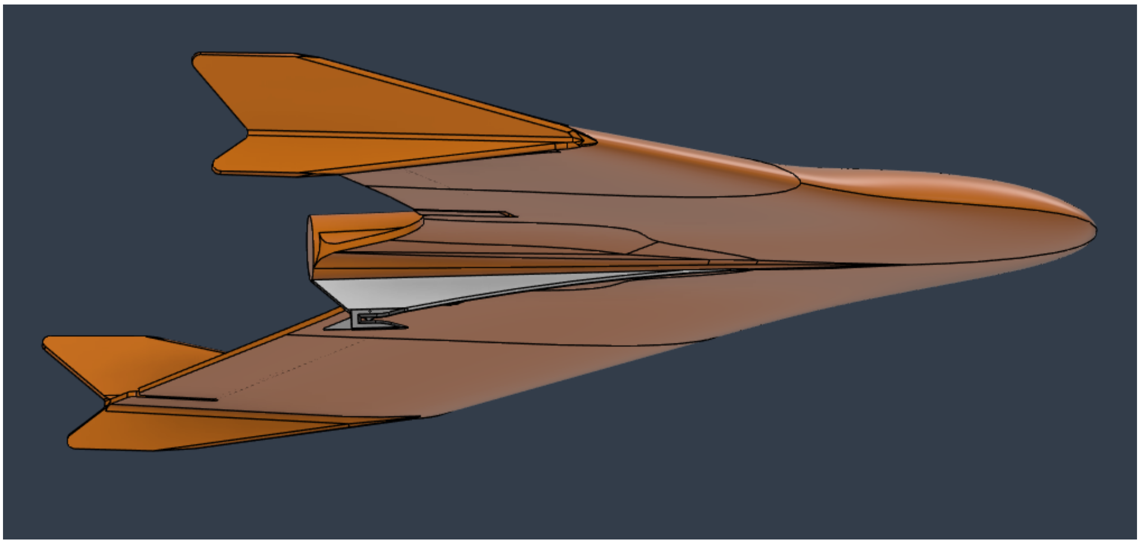

Figure 3.11: Hook mounted to the drone

From a manufacturing and integration perspective, the latch housing is intended to be produced using additive manufacturing, allowing rapid iteration of geometry and latch stiffness. PETG was selected as a suitable prototype material due to its balance of toughness, impact resistance, and ease of printing. The guiding ramp may be fabricated from lightweight foam material to minimize added mass and reduce the risk of structural damage in the event of unintended contact.

The locking mechanism, shown in figure 3.12, is designed to be passively actuated during capture and releasable after capture by pressing the back actuator, enabling autonomous unloading and redeployment of the drone in future system iterations. Although the release mechanism was not fully developed within the scope of this project, the latch concept provides a clear interface for further automation and system integration.

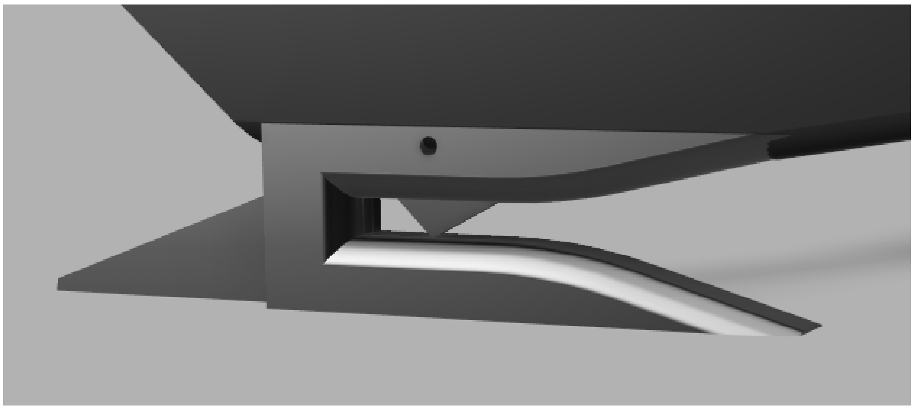

Figure 3.12: Closeup of the hook

3.7.3 Motor selection

The motor selection began by looking at a few different kinds of stepper motors and different gearbox solutions. A few different products where early on considered, including using worm drive gearboxes for self-locking functionality in the arms as well as large gear ratios.

The selection process was slowed down after a recommendation from the project examiner to contact a local company called Simplex Motion. The project initiator from SSRS also endorsed Simplex Motion as they already had helped develop other parts of the SSRS drone system. Since Simplex Motion already is a stakeholder in the project and their product catalog contains products that would work for the project. It was decided to limit the selection of motors and gearboxes to the Simplex Motion catalog.
After contacting Simplex Motion a meeting was held where motor dimensioning was discussed.

Dimensioning calculations for inertia matching of the motors is available in A.3, which served as the dimensioning factor for the motors.
The motor selection ended up resulting in a need for the SE020 motors with planetary gearboxes with a gearing ratio of 32:1 to get a maximum inertia ratio of 1:5.

The rotating base motors should not require any high speed operation and thus should only need to overcome the static friction of the rotating base The exact planetary gearbox ratio for the rotating base motor has not been calculated due to the uncertainty of exact friction coefficients. But the selected motor model is the Simplex Motion SE010. A rendered picture of the SE010 motor with a planetary gearbox is available in figure 3.13

Figure 3.13: Simplex Motion SE010 with a planetary gearbox, CAD render

4
Results

This chapter presents the outcomes of the design and development work carried out during the project. The results are primarily qualitative and design-oriented, as the project focused on concept development, mechanical feasibility, and prototyping rather than full-scale experimental validation or control system implementation. The final outcome of the project is a mechanically viable drone arrestment system concept, supported by CAD models, preliminary dimensioning, prototype testing, and analytical verification of critical components.
The results are structured around the final system design and the insights gained from iterative development, followed by recommendations for future improvements and continued development.

4.1 Final Design

The main result of this project is the development of a drone arrestment system concept based on a V-formation layout with independently actuated arms and a fixed hook–string capture mechanism. The final design builds upon earlier iterations and addresses key challenges identified during prototyping and analysis, particularly related to drone roll compensation, structural loading, and energy absorption during capture.

The final concept consists of a rotating base structure that allows the entire arrestment system to align with the incoming drone's approach direction. Mounted on the base are two independently controlled arm rotors, each driving a lightweight arm. A capture string is suspended between the arm tips and acts as the interception interface for the drone-mounted hook. Independent actuation of the arms enables dynamic adjustment of the string orientation, allowing compensation for roll angle variations observed during real flight testing.

A proof-of-concept control strategy was implemented to validate the geometric feasibility of the coordinate-based positioning approach described in Chapter 2. Using a simplified control setup with low-cost servos and microcontroller hardware, the system demonstrated the ability to position the string in height and roll angle according to commanded inputs. While the control implementation was not finalized, the tests confirmed that the underlying kinematic concept is viable.

From a mechanical perspective, the final design incorporates a modular shock absorption subsystem intended to decelerate the drone after capture over a distance of approximately one meter. Multiple energy absorption concepts were evaluated, with the constant-force band spring emerging as a compact and mechanically simple solution. Preliminary calculations and FEM simulations of critical components, such as the arm rotor brake discs, indicate that the design can withstand the expected load cases with conservative safety margins

Physical prototypes of the second and third design iterations were manufactured using additive manufacturing techniques. These prototypes were used to evaluate geometric constraints, assembly feasibility, and basic functional behavior. The third iteration prototype, featuring dual arm motors, was deemed sufficiently mature to serve as a baseline for further detailed design and system integration work.

Overall, the final design fulfills the primary project goal of delivering a mechanically feasible and conceptually validated drone arrestment system that can be integrated into a larger autonomous drone operation framework.

4.2 Future design recommendations

While the project successfully demonstrated the feasibility of the proposed arrestment system several areas were identified where further development is required before operational deployment.

One key recommendation is the development and testing of a robust control system integrated with the drones onboard flight controller. Although the geometric control principles were validated at a conceptual level, real time synchronization between drone state estimation and arrestment system actuation remains untested. Integration with MAVLink-based telemetry and closed-loop control would be necessary to ensure reliable capture under varying environmental conditions.

Further mechanical refinement is also recommended, particularly regarding shock absorption and damping. While the constant-force band spring concept offers advantages in compactness and simplicity experimental validation is required to evaluate its dynamic behavior, wear characteristics, and long-term reliability. Additional damping mechanisms may be needed to reduce post-capture oscillations.

Environmental robustness represents another important area for future work. Since the system is intended for maritime operation, corrosion resistance, wind loads, and exposure to moisture and saltwater should be considered in material selection and structural design.

Finally, full scale testing with a representative drone platform is essential to validate capture reliability, structural loading assumptions, and operational safety. Such testing would also enable quantitative performance metrics, including capture success rate, allowable approach corridor, and system response time, which were beyond the scope of the present project.

4.3 Mechanical Design

The final design is designed to be manufactured using standard machine shop equipment. The design is visible in a rendered CAD model in figure 4.1.

Figure 4.1: Final design

The majority of the parts are made from aluminium, with the parts that are subject to high stresses are manufactured from steel. The bearings are made mainly from POM (machinable plastic), as to allow for more freedom in dimensioning. Friction has overall not been taken into much consideration for this design, but there are a couple of possibilities for reduction of friction. Such as switching to brass/bearing bronze for the bushings or switching to ball bearings.

The rotation mechanism, visible in figure 4.2 is constructed in a way where the rotational axle is supported radially at two points by POM bushings that attached to the inside of the main structural leg of the prototype. The axial load is mainly handled by the top bushing. This axial force is transmitted through bolts that attach the main table to the rotational axis. And the table freely rotates on top of the top bushing.

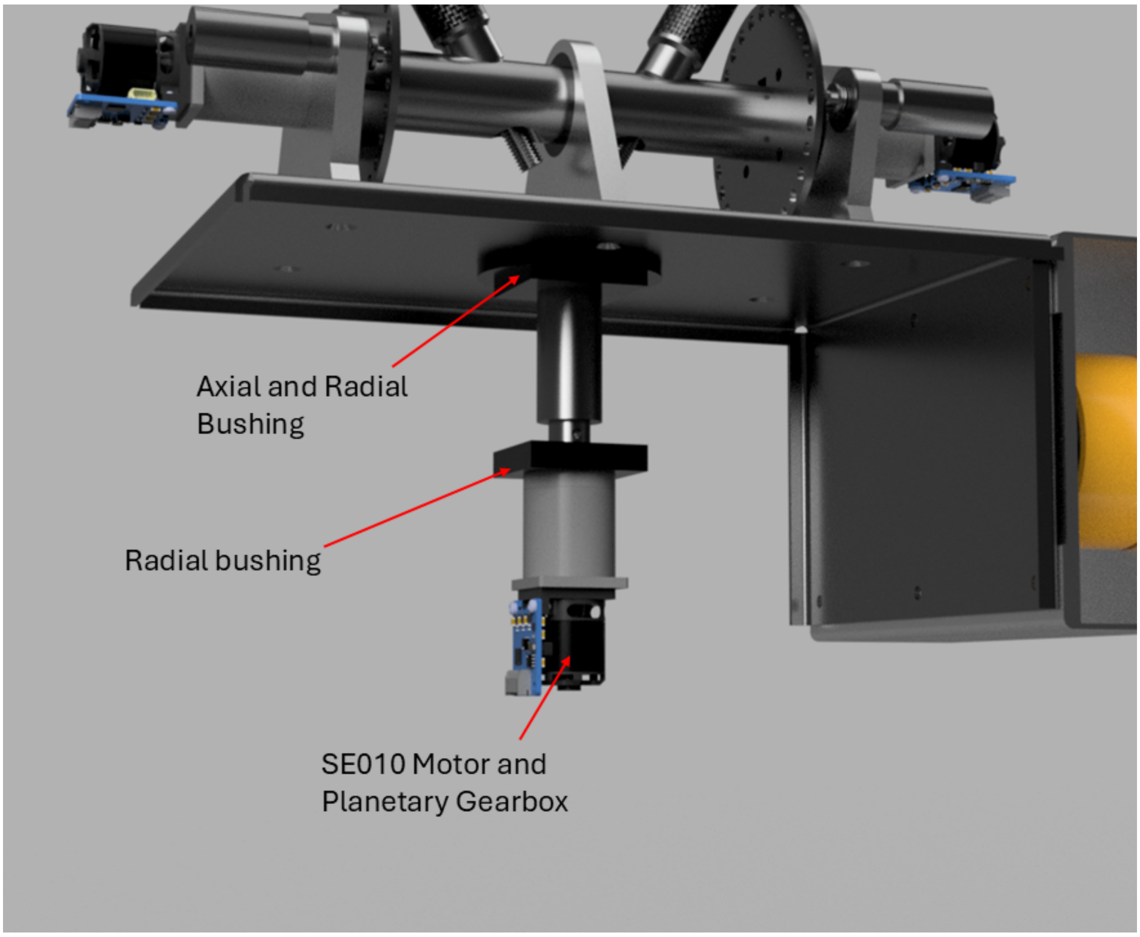

Figure 4.2: Rotation construction

The bottom bushing is made to attach the rotational motor package, and makes sure that the motor shaft is not loaded axially or radially. A cut section in figure 4.3 shows the stack up of the rotational motor package.

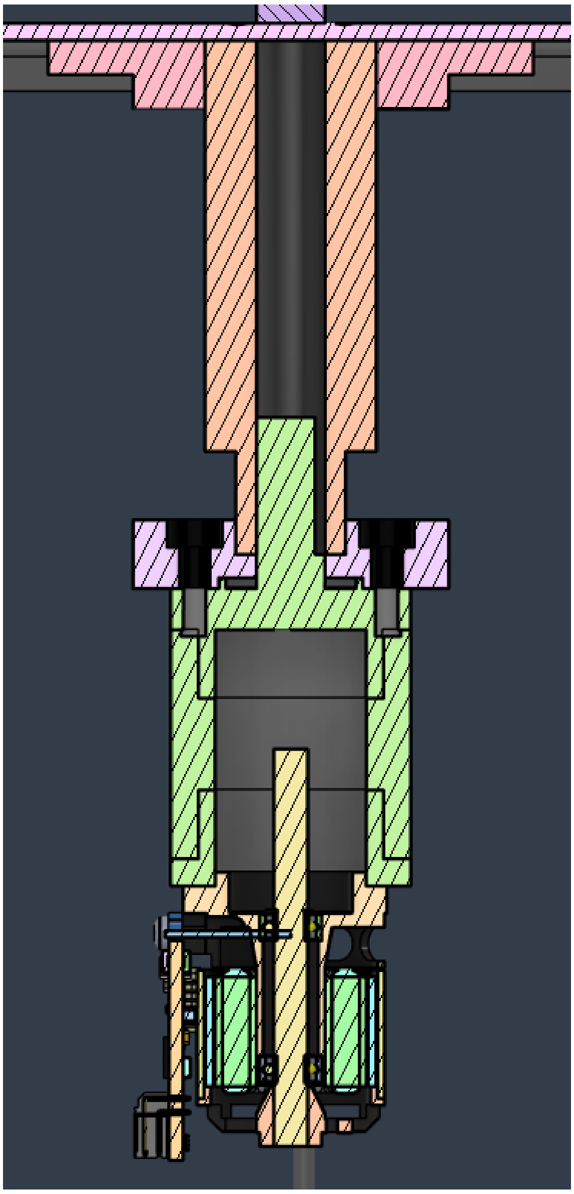

Figure 4.3: Section view of rotational mechanism

The peripheral linking from the motor to the rotor is made using grub screws onto the D-shaped shaft on the motor.

The arms are attached to the main table by aluminium bearing blocks, with POM bearings pressed into them. As shown in figure 4.4, the outer bearing blocks also house the solenoids that are used for braking. The brake discs are attached using a clamp connection with a keyed joint, which are screwed to the brake disc using four screws.

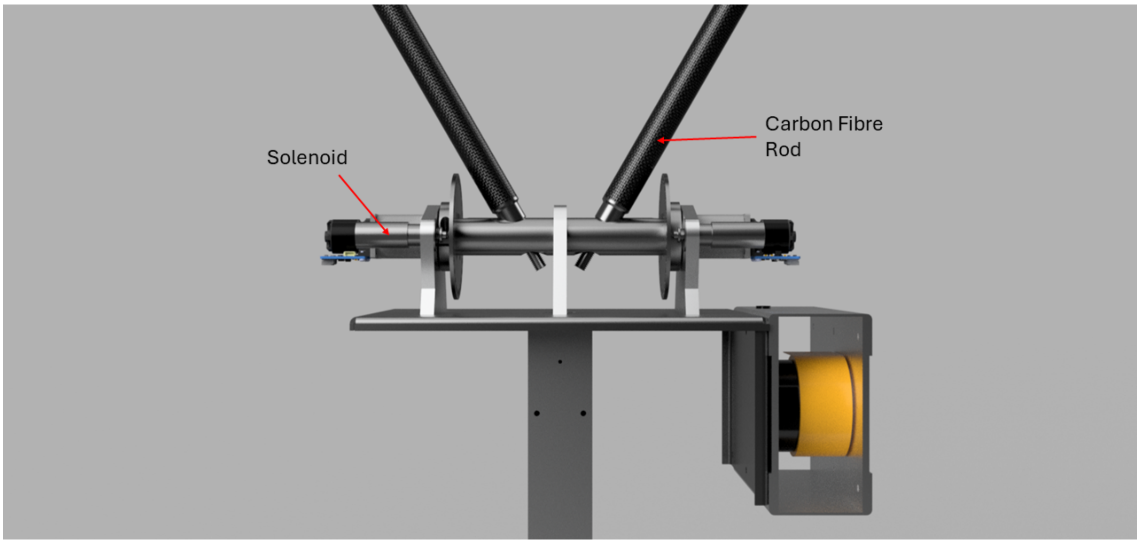

Figure 4.4: Picture of arm mechanism

The arms are attached by an insert, a cut section view of which can be seen in figure 4.5 that is glued into the carbon fiber rods after it has been tightened through the arm rotors using a M10 nut.

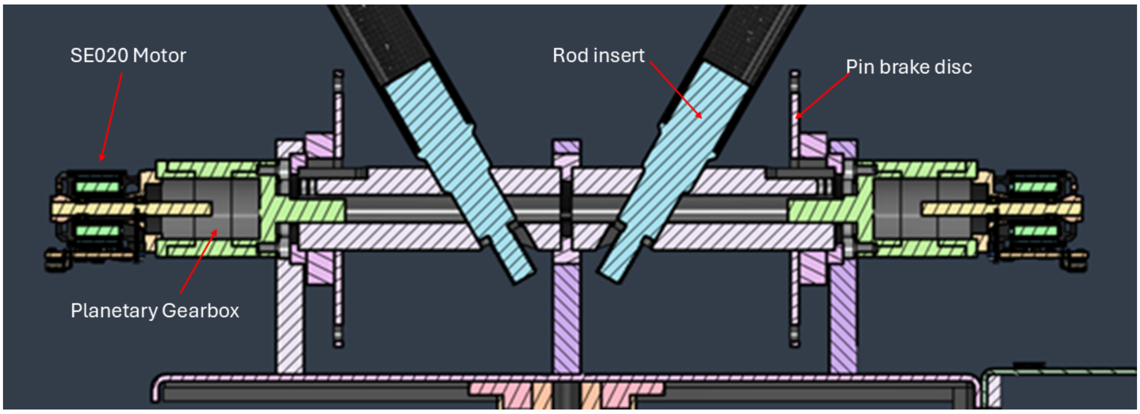

Figure 4.5: Section view of the arms

The string is routed through a POM string runner 4.6 through the top of the band spring enclosure. The string then is routed through a POM bushing that is glued into the top of the carbon fiber rods shown in figure 4.7.

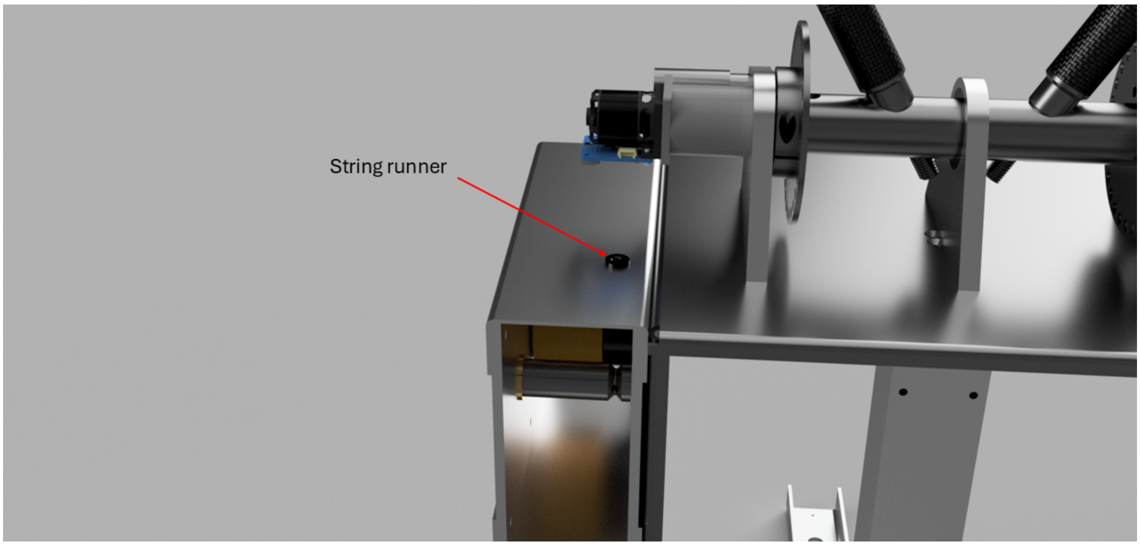

Figure 4.6: Band spring enclosure with string runner shown

This bushing also acts to make sure water does not fill up the carbon fibre rods. The string is then attached at the top of the second arm top bushing. These are identical, so the string will just be tied into a knot on the bushing furthest away from the band spring enclosure.

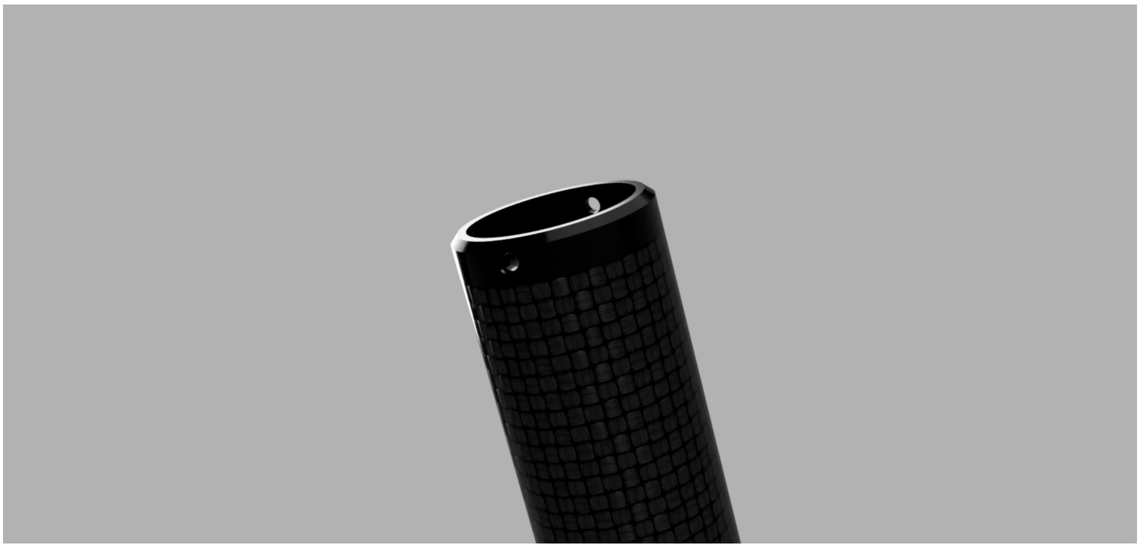

Figure 4.7: Arm top bushing

4.4 Cost and Bill of Materials

Since this project mainly aimed to design a prototype design that could be used for further refinement and iteration, a bill of materials and cost projection was made in table 4.1. The intent of this BOM is to be able to give an indication for the cost of building the current system prototype. Which could act as a basis either for comparison between other concepts or as a basis for decision-making about building a full scale prototype for testing or if further work is needed to refine the design.

Table 4.1: Bill of Materials with approximate costs

Part	Amount	Price/amount, SEK	Total cost, SEK	Description
Bought Components				
Simplex Motion SE020	2	3250	6500	Arm servo motor
Simplex Motion SE010	1	2750	2750	Rotating base motor
RS PRO Linear Solenoid, 24VDC	2	350	700	Brake actuators
71N Constant Force band spring	1	880	880	Shock absorption
Band spring bearing	1	200	200	Bearing bushing for band spring
Woven carbon fiber tube 2000mm 24-22 diameter	2	900	1800	Arm rods
Braided Fishing line 0.39mm 29kg rating	1	250	250	Catching string
Spiral tent screw 4pcs	1	50	50	Fastening to the ground
Steel wire lock	10	2	20	locking stiffening wires
Steel wire 3mm thick 1m	10	9	90	Stiffening wire
Jacking screw	4	30	120	tightening stiffening wire
Materials				
SS2511 35$\varnothing mmroundstock600mm$	1	750	750	Arm rotors, arm inserts and base rotor
10mm 6082-T6 flatrod 100x500mm	1	225	225	bearing blocks
50x50mm 2mm thickness 6060 aluminium square tube	1	600	600	base and feet
POM 10mm sheet 100x400mm	1	300	300	Big bushings
POM turning set 50-40-30 250mm	1	300	300	General bushings
3mm 5754 Aluminium sheet 2000x1000mm	1	1350	1350	Aluminium bending parts
3mm steel sheet 2000x1000mm (S355 or S235)	1	1100	1100	Rotation table
Electrical Components				
Telemetry Radio	1	550	550	Telemetry communications
ESP32	1	140	140	Suggested microcontroller
12V motorcycle battery lead acid	4	150	600	Power source
Miscellaneous electrical components	1	500	500	solder boards, wires, resistors etc
Total cost			19775	

5
Conclusion

This thesis has investigated the feasibility of an autonomous mechanical arrestment system for fixed wing drones, intended to support future maritime operations conducted by the Swedish Sea Rescue Society. The primary objective was not to deliver a finalized operational product, but to develop and evaluate a mechanically sound test platform concept capable of informing further development through real world testing.
A capture strategy based on a drone-mounted hook and a ground-based string interception mechanism was selected as the most suitable solution given the constraints of the existing drone platform. Through iterative concept development, the arrestment system evolved into a V-formation layout with independently actuated arms, enabling compensation for roll motion observed during flight testing of the flying wing drone. This capability was identified as critical for robust capture, given the sensitivity of the hook to string interface to roll misalignment.

A simplified kinematic model was developed to describe the relationship between drone state parameters and arrestment system geometry. This model formed the basis for a proof-of-concept control implementation and demonstrated that real-time positioning of the capture string in height and roll angle is geometrically feasible. Although the control system was not fully developed or validated, the results confirm that the proposed mechanical architecture is compatible with future closed-loop control integration.

Several energy absorption concepts were evaluated to manage the high kinetic energy present during the arrestment event. A constant-force band spring solution was selected due to its compactness, mechanical simplicity, and predictable force characteristics. Preliminary analytical calculations and structural simulations of critical components indicate that the proposed design can withstand expected load cases with conservative safety margins, supporting the mechanical viability of the concept.

Overall, the project successfully meets its stated goals by delivering a coherent and technically grounded arrestment system concept. The work provides valuable insights into key design challenges, including roll compensation, load management, and system integration constraints. While significant work remains before operational deployment, particularly in the areas of control system development, environmental robustness, and full scale testing the presented results establish a solid foundation for continued development and experimental validation of autonomous drone arrestment systems.

Bibliography

[1] Real Engineering, *Zipline - How Rwanda Built A Drone Delivery Service*, Jan. 2019.

[2] K. Björk, *Formler och tabeller för mekanisk konstruktion / Karl Björk.* swe, 9. upplagan. Karl Björks förlag HB, Jan. 2022. [Online]. Available: https://research.ebsco.com/linkprocessor/plink?id=3e0e4de8-3aeb-31a2-af54-264e6cbcc759.

A

Appendix

A.1 Overall concept layout development

A.1.1 Pre-study of existing solutions

A.1.1.1 Zipline

The main existing solution that the project was based around was the drone delivery system by the company Zipline, which is used to deliver medical supplies in rural areas. The system uses autonomous drones that are launched and then recovered using a string and hook on a plane. The system uses two big triangulated pillars that are rigidly mounted to the ground. At the top of the pillars there are two motors with arms attached to them with a string in between. The motors seem to always spin at the same speed and keep both arms parallel at all times. The string seems to be able to extend further after catching the drone, probably to decelerate the drone.
The hook on the drone is placed downwards at the very rear of the drone, while the propellers and control surfaces are placed on the top of the drone, this should give the string the possibility to slide along almost the entirety of the belly of the drone, which should allow for a bigger target to aim for when catching the drone. The wings are placed very far up from the belly of the drone which also means that the risk of hitting one of the wings when catching the drone should be very minimal.
The system uses "Military grade GPS" [1] to track the location of the drone, which the drone catcher uses to perform the catch.

A.1.1.2 Boeing SkyHook recovery system

The Boeing SkyHook recovery system uses a launcher similar to the Zipline system, but the main difference is the way that the drones are caught. The Boeing SkyHook uses one vertical thin pillar with a vertical string. The string does not seem to be movable, instead the drone simply flies into it. The hook on the plane is attached to the tip of the wings, possibly both wings could be used, but for operation only one hook is neccessary. To capture, the drone only needs to fly closeby to the string with one wing, and as the string is hanging with sufficient clearance to any structure, including the pillar itself. The hook can catch on the string causing it to be caught. However simple it is, the system does not seem very predictable as the drone flails around unpredictably after being caught, the system also seems like it would cause a lot of stress on the frame of the drone. The main positives of the system is the simplicity, While the simplicity also is the main negative as it creates a unpredictable system.

A.1.1.3 Heishatech F200

Drone docking system with little available information of how the catching mechanism would work, with only renderings available. The model looks to work very similarly to how the Zipline solution works, but also has an autonomous docking system for autonomous charging and redeployment of the drone. The system seems to have some kind of hook on top of the drone, which can be used to both catch and then release the drone, to allow for further handling of the drone.

A.1.2 Evaluation and integration of existing concepts

A.1.2.1 Zipline

The Zipline solution looks like a very good and promising layout for the application. But it still has a few problems for integration with the SSRS drones. The placement of the hook becomes a big problem for the SSRS drones, as the propeller sits a bit behind the center of mass of the drones. The propeller in this case would be in the way of the string if it was placed behind it. This means that damage to the motor and propeller would be a big risk, meaning that it would need to be placed in front of the propeller. This means that the belly area of the plane available to hit the string on would be much smaller than ideal. Another problem is that the wings are close to being on the same vertical axis plane as the belly of the drone. Meaning that just a slight roll angle offset would cause the string to hit the wing instead of the belly of the drone. Potentially causing damage or a crash.

A.1.2.2 Boeing SkyHook recovery system

This system is quickly ruled out, as the SSRS drones have magnetically fastened wing tips. Meaning that they made to break away easily to lessen damage to the main airframe in case of a crash or similiar. The system also gives an unpredictable state of the drone once caught, which would make it difficult to set it up for further autonomous handling.

A.1.3 Further Development of layout concept

A.1.3.1 Parallel pillar layout

The First layout considered was a similar concept to that of the Zipline design, with two pillars with motors on top controlling two arms and with a string in between. SSRS informed that the lowest usable air speed of the drone is 12m/s, by doing quick calculations taking into consideration the size of the drone and the speed, see appendix A.4.2 it was determined that adding the possibility of rotating the base of the catcher would be beneficial. Another problem of not being able to rotate the base of the catcher is that a sidewind would cause the control system of the drone to force the drone into a roll angle to steer it straight, this would make it hard to

catch the drone without hitting the wing.
Having the ability to rotate the base was considered and led to the next iteration of the concept. As the main drawbacks of this design is that it would require a big motor and a lot of support to spin around, as there is a lot of strength required to support the motors and arms to catch the drone. Which places the weight very far up and away from the rotating center of the catcher.

A.1.3.2 V-formation single motor arms layout

To get away from the problem of having a lot of weight far from the rotating base a new concept was considered.
This concept uses a small base which houses the arm motor, which in this case can be reduced to one, along with one arm axle where two arms can be mounted. The positive part is that the weight far from the rotating center can be reduced as well as the amount of rigidity required.As the arms could be made light either by making a lightweight geometrically stiff arm design or using a high performance material such as carbon fibre rods. Some drawbacks of the concept is that the base would need to be lifted off the ground as the drone would risk hitting the ground otherwise. Another drawback is that the arms would be more subject to bending forces which would need further considerations, see appendix A.2.2.
It was also at this point where the problem of a constant sinusoidal roll angle was realised. This caused a new iteration. As the problem of roll angle would require longer hooks, which would weigh more and lead to more out of plane forces, requiring further reinforcement of the hook.

A.1.3.3 V-formation double motor arms layout

The final iteration of the layout resulted in splitting the arm rotor axle into two coincident axles, each driven by a motor. This allows the arms to be individually controlled, allowing for roll of the plane, while still keeping the weight close to the center of the rotating base.

A.2 Structural Calculations and FEM simulations

A.2.1 Dowel Pin Brakes

The dowel pin brakes work by pushing a pin into a disc that has several holes evenly distributed around its perimeter. The first calculation is to determine the force and moment reactions in the brake disc. The brake disc is directly mounted to the arm rotors. The worst load case for the brake discs will be when the arms are standing fully upright when the drone is caught. It will be assumed that the rotational speed at the point of loading will be zero and also assume that the load is completely along the rotational plane of the arms, but equally distributed between both arms.
This should result in a conservative estimate of the force that the brakes will need to withstand, as the composants from the string will never be fully in line with the rotational plane of the arms.

The force in each arm will be the constant spring force $F_{\text{arm}} = 71N$
The moment reaction of the arm rotor will be the Z-axis distance from the arm rotor to the top of the carbon fibre rod, which will be around $l = 1.4m$ leading to a moment reaction of $M_{\text{armrotor}} = l \times F_{\text{arm}} \Rightarrow 1.4m \times 71N = 99.4Nm \approx 100Nm$ From the middle of the armrotor out to the pin holes on the brake disc, as shown in figure A.1, the distance is $l_{\text{pinhole}} = 0.045m$

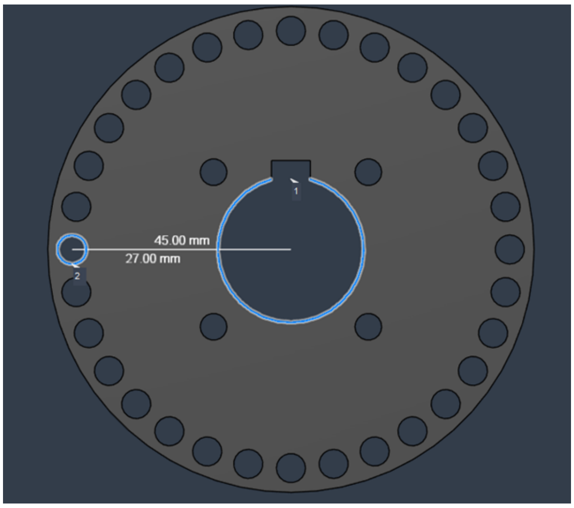

Figure A.1: Picture showing distance between arm rotor center and pinholes in brake disc

Leading to a reaction force in the pin hole of $F_{\text{pinhole}} = \frac{M_{\text{armrotor}}}{l_{\text{pinhole}}} \Rightarrow \frac{100Nm}{0.045m} = 2222N \approx 2200N$
To calculate the macroscopic von mises equivalent stresses around the pinhole a FEM simulation is made using Ansys Mechanical. The boundary conditions used are a bearing load on of the holes in the peripheral direction of 2200N and a fixed support in all of the 4 bolt holes in the disc the boundary conditions shown in figure A.2.

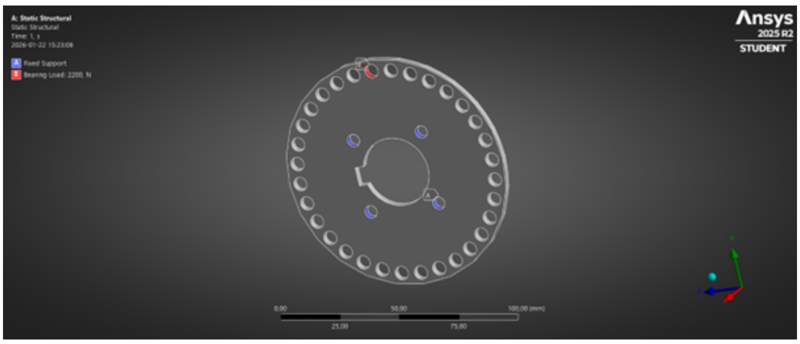

Figure A.2: Boundary conditions of the brake disc simulation

The resulting von mises stresses amounted to around 300 MPa after running a convergence analysis set to a maximum allowable change of 5% the stress concentrations are available in figure A.3.

The deformation is not included here as it is not very important for the use case. An assumption to be made is that the discs are made from S355 steel as it is a cheap and common steel, most types of construction steels are safe for use, but could lead to premature failure due to surpassing the yield strength. The calculation is still very conservative, as the base load case should not be useful for operation of the prototype, and is a much more severe load case than normal operation would result in.

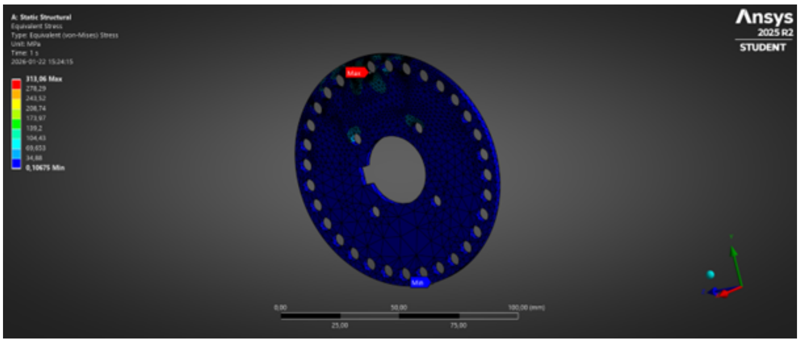

Figure A.3: Von Mises equivalent stress of the brake disc

To calculate the dimensioning tolerances of the pin and pin hole fit a calculation using the maximum allowable Hertzian stress between the two bodies will be made. The Hertzian stress between a convex against a concave cylinder is calculated as:

$$p_0 = 0.418 \times \sqrt{\frac{F \times E}{L}\left(\frac{1}{r_1} - \frac{1}{r_2}\right)} \tag{A.1}$$

Rearranging for the pin radius:

$$r_1 = \frac{1}{\frac{1}{r_2} + \frac{L}{F \times E}\left(\frac{p_0}{0.418}\right)^2} \tag{A.2}$$

Inserting the values, assuming the stiffness of steel to be 210 GPa and the maximum allowable Hertzian stress of the S355 (SS2132) of 800 MPa [2] assuming a static load.

$$\frac{1}{\frac{1}{0.003} + \frac{0.003}{2200 \times 210 \times 10^9}\left(\frac{800 \times 10^6}{0.418}\right)^2} = 0.0028 = 2.8mm \tag{A.3}$$

The minimum diameter of the pin will be $2.8mm \times 2 = 5.6mm$ For the sake of completeness the stress of the pin will be calculated:

$$\frac{F_{\text{pinhole}}}{r_{\text{pin}}^2 \times \pi} \rightarrow \frac{2200N}{2.8^2 mm \times \pi} \approx 89.3MPa \tag{A.4}$$

A.2.2 Glue joint

A critical interface of the mechanical design in the final concept is the glue joint between the driven axle and the carbon fiber arm. Since adhesive joints are generally among the weakest elements in mechanically loaded assemblies, this interface was investigated to determine whether the solution is feasible for the expected load cases. The initial joint geometry was selected based on preliminary experience and packaging constraints, but was later identified as a candidate for improvement. An overview of the stress distribution in the arm and joint region under the worst assumed load case is shown in Figure A.4.

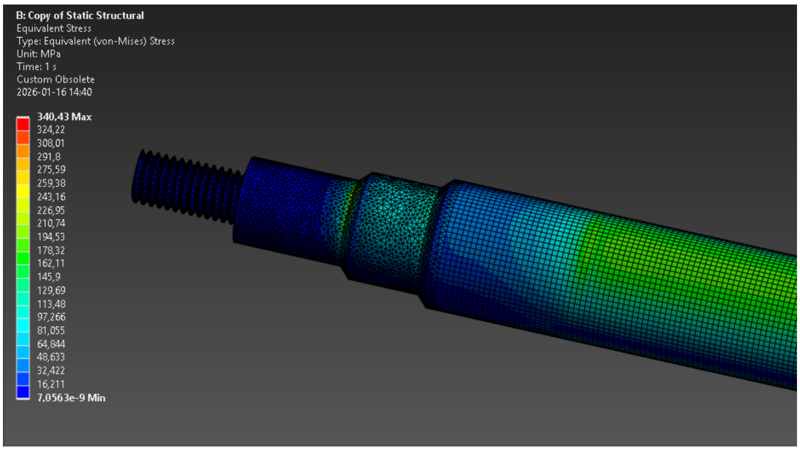

Figure A.4: Von Mises equivalent stress of the entire arm in worst load case

A suitable adhesive for this application is Loctite EA9514, which was selected due to its high shear strength, good tensile strength, and particularly favorable performance under dynamic and shock loading conditions. These properties make it well suited for joints subjected to transient loads rather than purely static loading.

Since the adhesive joint is primarily loaded in bending, significant stress concentrations arise at the outer edge of the bonded region, where the bending moment is highest. This behavior is typical for bonded cylindrical joints subjected to transverse loading and is clearly visible in the stress distributions obtained from the finite element analysis.

To mitigate these stress concentrations, two geometric improvements were identified. First, the bonded overlap length can be increased, which reduces peak stresses by distributing the load over a larger adhesive area. Second, a supporting steel lip can be added at the outer end of the joint. This lip provides partial mechanical support and reduces local bending of the adhesive layer, thereby lowering both shear and normal stresses in the most critical region.

Figure A.5 shows the von Mises equivalent stress distribution within the adhesive layer, while Figures A.6 and A.7 illustrate the corresponding shear and normal stress components. The results indicate that shear stresses dominate the adhesive loading, as expected for a bending-driven joint, while tensile normal stresses are concentrated near the outer edge of the bond. By extending the joint and introducing a steel support lip, these peak stresses can be significantly reduced, improving the robustness of the connection.

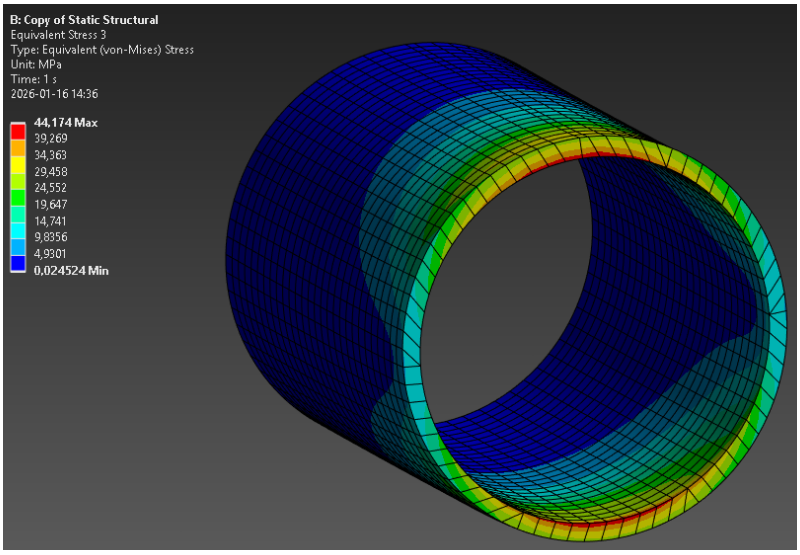

Figure A.5

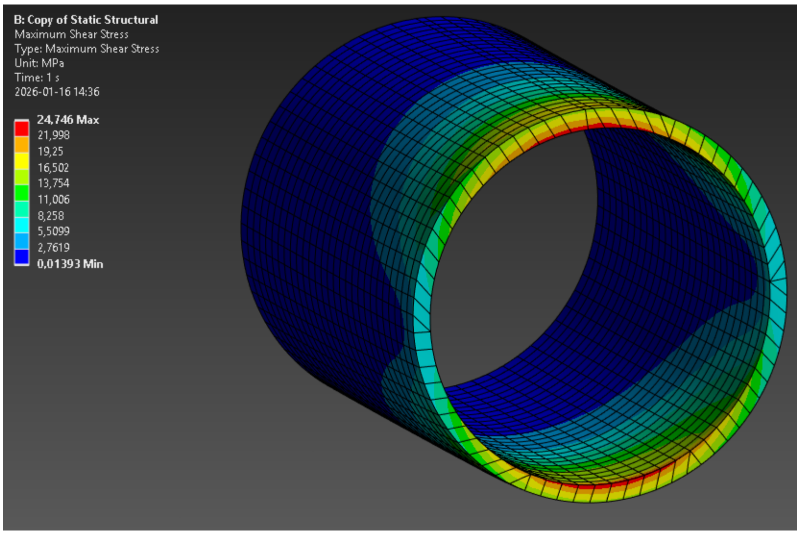

Figure A.6

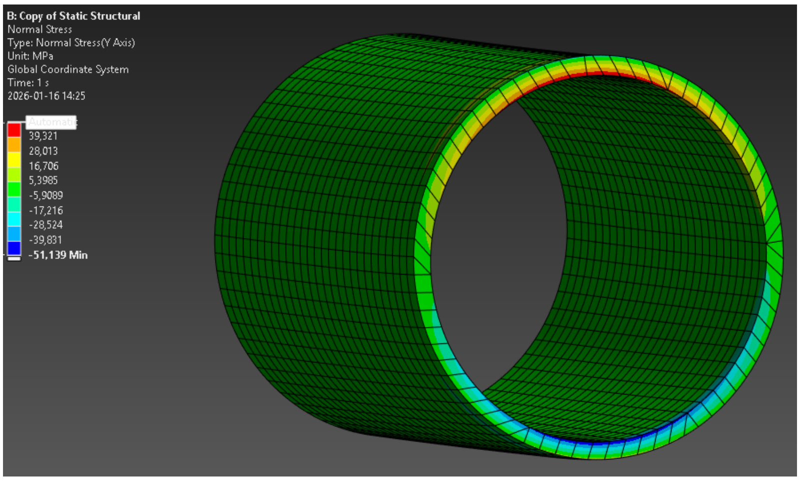

Figure A.7

Although the analysis is based on simplified assumptions and ideal bonding conditions, the results suggest that a properly dimensioned adhesive joint is a viable solution for the arm–axle interface in the proposed design. Further experimental testing is recommended to validate the numerical results and to assess the influence of manufacturing tolerances, surface preparation, and cyclic loading on long-term joint performance.

A.2.3 Band Spring Dimensioning

To decide the force and length of the band spring, the absorbed energy formula described in 2.1.2 will be used to determine the energy to be absorbed.

$$E_k = \frac{1}{2}mv^2 \rightarrow \frac{1}{2}1kg \times 12^2 m/s = 72J$$

To determine the spring force required the spring displacement over one meter of travel for the drone after being caught by the string will be calculated.

First the approximate length of the baseline string will be measured in the CAD-model in figure A.8.

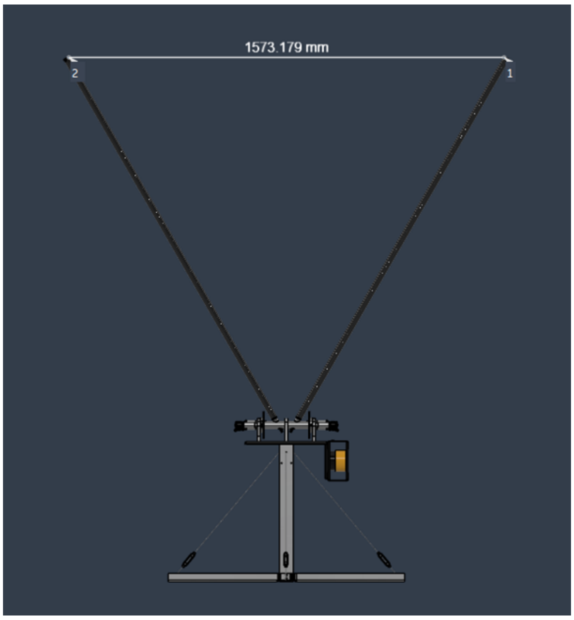

Figure A.8: Length of the string non displaced

The length of the string when it is fully at rest is approximately $l_{\text{string}} \approx 1600mm$

Next we will calculate the amount of string/band spring displacement required for a drone travel of one meter.
The string at one meter of drone displacement can be calculated like an isosceles triangle. For simplicity CAD-software is used for the trigonometric calculations in figure A.9

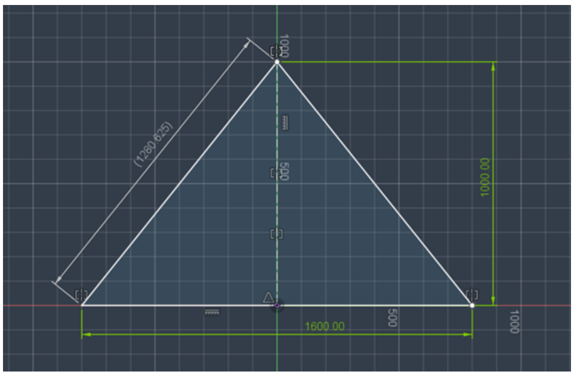

Figure A.9: Displaced string triangle CAD-software picture

As the CAD-drawing describes the length of the string after displacement will be $l_{\text{displacedstring}} = 2 \times 1260mm = 2520$ We now need the displacement of the string which will be $\Delta l_{\text{string}} = l_{\text{displacedstring}} - l_{\text{string}} \rightarrow 2520mm - 1600mm = 920mm$ Mechanical work can be calculated by the force times distance, this should be equal to the potential energy stored in a constant force spring. The force rating of the spring can then be calculated by

$$F_{\text{spring}} = \frac{E_k}{\Delta l_{\text{string}}} \rightarrow \frac{72J}{0.92m} = 78N$$

The spring would need to have a force rating of 78 N to be able to stop the drone in one meter at a speed of 12 m/s. In the BOM for the project a band spring rated at 72 N has been recommended since there is friction in the system that has not been accounted for as well as the fact that 12 m/s should be around the maximum impact speed seen during use.

To determine the length of the band spring the angle of the arms against each other needs to be accounted for.
To begin with, the band spring needs to allow for at least 920mm of displacement for deceleration of the drone. After this we will look at the maximum angle of the system, which would be 90 degrees offset between the arms, shown in figure A.10.

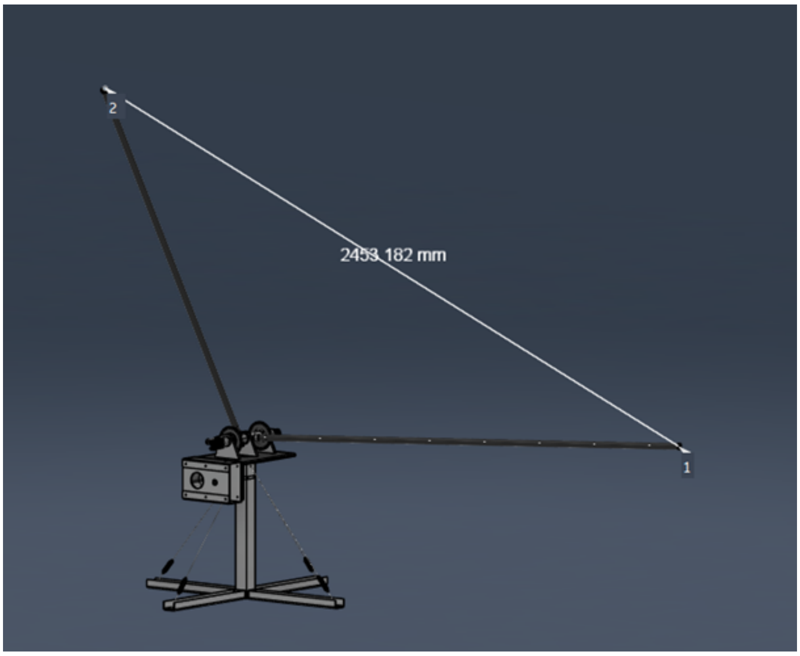

Figure A.10: CAD measurement off 90 degree offset of the arms

The string length at the 90 degree offset point would be about $l_{90\text{string}} = 2450mm$ The displacement of the band spring would then be $\Delta l_1 = l_{90\text{string}} - l_{\text{string}} \rightarrow 2450mm - 1600mm = 850mm$ The total displacement would then be catching the drone at 90 degree offset, which would be $\Delta l_{\text{string}} + \Delta l_{\text{string}} \rightarrow 920mm + 850mm = 1770mm$

The total band spring displacement should then be at least 1770mm, but it would be advisable to increase this to over 2000mm.

A.3 Inertia Matching Between Motor and Load

For the motor inertia calculations we got some information from Simplex Motion that the inertia has to be matched between the motors and the arm.
Since gearboxes are evaluated for cheaper smaller motors we can match the inertia

just by multiplying with the gear ratio. To evaluate what gear ratio is to be used (and feasible) we started by looking at two of the smaller motors from simplex motion (based on a gut feeling tip by Simplex Motion). The inertia of these two motors is 3.43 E-6 kgm2 12.60 E-6 kgm2 respectively. The inertia of the arm assembly is 0.2 kgm2. So to match it we have a gear ratio of approximately 241 for the small motor and 126 for the big motor. The load inertia is

$$I_{\text{load}} = 8 \times 10^7 \text{ gmm}^2 = 0.08 \text{ kgm}^2. \tag{A.5}$$

The SE020 motor rotor inertia is

$$I_m = 12.6 \times 10^{-6} \text{ kgm}^2. \tag{A.6}$$

Reflected load inertia through a gearbox with ratio $N : 1$ is

$$I_{\text{ref}} = \frac{I_{\text{load}}}{N^2}. \tag{A.7}$$

For perfect inertia matching $I_{\text{ref}} = I_m$:

$$N \approx 80. \tag{A.8}$$

For a maximum mismatch of 5:1:

$$\frac{I_{\text{ref}}}{I_m} = 5 \quad \Rightarrow \quad N \approx 36. \tag{A.9}$$

A.4 Dynamic Motion Calculation with 36:1 Gear Ratio

We compute the time required to rotate the arm by 10° at a radius of $r = 1300\,\text{mm}$.

A.4.1 Arc Length

$$s = r\theta, \qquad \theta = 10^\circ = 0.1745 \text{ rad}. \tag{A.10}$$

$$s = 1.3 \cdot 0.1745 \approx 0.227 \text{ m}. \tag{A.11}$$

A.4.2 Angular Acceleration and Time

Peak torque at the arm (assuming 90% gearbox efficiency):

$$T_{\text{peak}} = 0.5 \text{ Nm} \cdot 36 \cdot 0.9 \approx 16 \text{ Nm}. \tag{A.12}$$

Arm angular acceleration:

$$\alpha = \frac{T}{J} = \frac{16}{0.08} = 200 \text{ rad/s}^2. \tag{A.13}$$

For a triangular velocity profile:

$$t = 2\sqrt{\frac{\theta}{\alpha}} = 2\sqrt{\frac{0.1745}{200}} \approx 0.06 \text{ s}. \tag{A.14}$$

Thus, a 10° movement takes approximately 0.06 seconds using peak torque.

DEPARTMENT OF SOME SUBJECT OR TECHNOLOGY
CHALMERS UNIVERSITY OF TECHNOLOGY
Gothenburg, Sweden
www.chalmers.se

CHALMERS
UNIVERSITY OF TECHNOLOGY